POLAROGRAPHY OF THE COMPLEXES OF Cd(II), Co(II), AND Ni(II) WITH THREONINE

A Thesis

Presented to

The School of Graduate Studies

Addis Ababa University

In Partial Fulfillment

of the Requirements for the Degree of

Master of Science in Chemistry

by

Alebachew Demoz

June 1983

Table of Contents

Table of Contents

Table of Contents

Acknowledgments

It is my pleasant duty to record my indebtdness to my advisor Dr. Theodros Solomon, without whose unwaning patience, persuasion and guidance this work would not have materialized. Most of all I have availed my self of his examplary welcome to open discussions of any degree.

I wish to express my thanks to Kebede Besha who did the pioneering work of this project with Dr. Theodros, Dr. Berhanu Abegaz and Habetamu Zewdie for supplying me with reprints. Abdo De-Tango, Yilma Tamiru and collegeous of the department have been helpful in their own ways.

I also wish to express my gratitude to all my friends, particularly, Wakgari Hirpo, Gizachew Alemayehu, Mengistu Legesse, Tefera Worku, Hailemichael Alemu, Bekuretsion Kassahun and Etalem Engeda for their constant encouragement.

Financial support from the Swedish Agency for Research Cooperation with the Developing Countries (SAREC) obtained through the Ethiopian Science and Technology commission and from the Addis Ababa University which was used to cover the expenses incurred in the research work undertaken and in the preparation of this dissertation is greatefully acknowledged.

List of Figures

List of Tables

List of Symbols

$\alpha_{(H)}$ = Protonation side reaction coefficient.

β = Overall stability constant.

C_j = Bulk concentration of the j^{th} species.

C_j^o = Concentration of the j^{th} species at the electrode surface.

C_x = Free lingand concentration.

D_c = Mean diffusion coefficient of complex.

D_m = Diffusion coefficient of the simple metal ion.

E = Electrode potential.

E^o = Formal electrode potential.

$E_{1/2}$ = Half-wave potential.

E_p = Peak potential.

F = Faraday's constant.

f_j = Activity coefficient of the j^{th} species.

g = Gravitational acceleration constant.

$[H^+]$ = Hydronium ion concentration.

i_a = Limiting adsorption current.

i_c = Limiting cataliytic current.

i_d = Mamimum diffusion current.

$\bar{i}_d$ = Mean diffusion current.

i_k = Limiting kinetic current.

K_a = Acid dissociation constant

K_b = Rate of backward chemical reaction.

K_f = Rate of forward chemical reaction.

K_i' = The i th protonation constant.

k_j = Stepwise stability constant.

K_j = Stepwise overall stability constant.

l = Capillary length.

M = Rate of mercury flow.

M^{+n} = Simple metal ion.

n = number of electrons exchanged.

n = Vicosity coefficient of mercury.

P = Difference in hydrostatic pressure. at the tip of the capillary.

P = Ligand number

q = Charge at the electrode.

r = Radius of mercury drop,

t = Life of mercury drop.

[thr] = Analytical threonine concentration.

$[thr^-]$ = Threoninate concentration.

t_{max} = Maximum mercury droptime.

Γ = The number of moles of adsorbed substance per unit surface area.

ρ = Density of mercury.

$W_{1/2}$ = Peak half width

[X] = Total ligand concentration.

Abstract

The polarographic behaviour of the complexes of threonine with Cd(II), Co(II), and Ni(II) have been studied in borate buffer at 25°C. The DC polarographic reduction of the Cd(II)threonine system has been found to be reversible and therefore amenable to the Deford-Hume method for the determination of stepwise stability constants. These constants have been found to be log k_1 = 3.1 and log k_2 = 2.57 for the first and second stepwise stability constants, respectively.

The reduction of the Co(II) - threonine system was investigated using differential pulse polarography. A single polarographic wave which is found anodic to the simple metal ion reduction potential was observed. This wave was dependent on the concentration of threonine, which suggests a possible use of this system for the polarographic determination of the ligand. It also suggests that the reduction of the Co(II) - threonine complex is catalytic in nature. .

The differential pulse polarographic study of the Ni(II) - threonine system revealed the occurrance of a prewave and also of a second wave which are found anodic to the simple metal ion reduction potential. Both waves are strongly dependent on the concentration of the threonine and the prewave can be used for a polarographic determination of the ligand. A mechanism has been proposed to explain the nature of reductions.

1. Introduction

The polarographic behaviour of Co(II) and Ni(II) complexes of threonine have not so far been studied. Stepwise stability constants of cadmium - threonine system have not been evaluated. There exist two reports on the Cd(II) threonine complexation, one by the polarographic method (9) and another by the potentiometric method (10) in which the overall stability constant is only reported. Rawat and Gupta (9) considered the analytical threonine concentration as the free ligand concentration, which in this work is shown to be incorrect from the pH dependence study, and as their media was not buffered in addition to having a maxima, a well buffered supporting electrolyte and an improved analysis is made. It is the task of this work to study the polarographic behaviour of Co(II) and Ni(II)-threonine system and produce the stepwise stability constants of Cd(II) - threonine complexes. The basis for the stepwise stability constants, the method of recognition of several electrochemical rate limiting steps using polarography have also been discussed.

2. Theory

In general for an overall electrode reaction

$$Ox + ne \rightleftharpoons R \qquad (1)$$

the electrochemical reaction rate is governed by any of the following processes:

1. Mass transfer towards the electrode surface.
2. Electron transfer at the electrode surface.
3. Chemical reactions preceding or following the electron transfer.
4. Surface reactions, such as adsorption, desorption etc.

The polarographic limiting currents of 1 and 2 are controlled by the rate of mass transfer, i.e., diffusion. In the case where step 3 is the rate controlling process, the original species, or another electroactive species, may be regenerated by the reaction between the product of the electrode reaction and some other constituent of the solution. The solution can also contain a species that is not electroactive but is in slow equilibrium with one that is. Such rate limiting electrode processes are known as catalytic and kinetic processes respectively. The limiting current dependence on certain parameters has been extensively used as criteria for establishing rate controlling processes. Methods by which the rate controlling processes can be determined are presented below.

2.1. Diffusion Currents

The equation describing the mass-transfer controlled electrolysis at the DME was initially derived by Ilkovic (68). The equation dealing with the actual experimental conditions in polarography have to consider the spherical nature of diffusion at a growing mercury drop, the decrease of the depolarizer concentration in the neighbourhood of the moving electode, the non-centric growth of the drop during the outflow of mercury from the capillary, and the screening effect of the capillary glass on the electrode. Yet the above improvements made on the linear diffusion case are so insignificant, that the simpler less rigorous solution due to Lingane and Loveridge (69) is reproduced below. Several solutions taking into account the above conditions have been workedout. For such a discussion the reader is refered to the book by Galus (70).

At the diffusion limited portion of the polarographic wave, the Cottrell equation (equation 2) hold to a good approximation.

$$i_d = nFAC \left(\frac{D_{ox}}{\pi t}\right)^{1/2} \qquad (2)$$

where i_d is in amperes, F in Coulobms, A in Cm^2, D_{ox} in Cm^2 . $sec.^{-1}$, C in moles Cm^{-3} and t in seconds. The volume of mercury drop is

$$V = \frac{4}{3}\pi r^3 = \frac{mt}{\rho} \qquad (3)$$

$$\therefore r = \left(\frac{3mt}{4\pi\rho}\right)^{1/3} \qquad (4)$$

The surface area of the mercury drop

$$A = 4\pi r^2 \qquad (5)$$

Can be expressed using equation (4) as

$$A = 4\pi \left(\frac{3mt}{4\pi\rho}\right)^{2/3} \qquad (6)$$

Substitution into the Cottrell relation gives

$$i_d = nFC\ 4\pi \left(\frac{3mt}{4\pi\rho}\right)^{2/3} \left(\frac{D_{ox}}{\pi t}\right)^{1/2} \qquad (7)$$

The current observed in the case of a flat electrode moving in the direction of the solution is $(7/3)^{1/2}$ times larger than that observed in the case of a stationary flat electrode having the same surface area. Therefore a factor of $(7/3)^{1/2}$ measuring the contribution of convection to the diffusion transport is added to account for the progressively enlarging mercury drop electrode. Thus, evaluating the constants in equation (7), we have

$$i_d = 708\ nD_{ox}^{1/2}\ Cm^{2/3}t^{1/6} \qquad (8)$$

which is known as the Ilkovic equation.

The mean current during the droptime can be determined by integration of equation (8).

$$\bar{i}_d = \frac{\int_0^{t_{max}} 708\ nD_{ox}\ Cm^{2/3}\ t^{1/6} dt}{t_{max}} \qquad (9)$$

$$\bar{i}_d = 605\ nD_{ox}^{1/2}\ Cm^{2/3}\ t_{max}^{1/6} \qquad (10)$$

Both equations (8) and (10) show that for a diffusion controlled process the dependence of log i on log t should be linear and the slope of the straight line should be equal to 1/6. It follows from equation (10) that $m^{2/3}t_{max}^{1/6}$ is a constant, characteristic of the capillary. The Poiseuille equation is

$$V = \frac{\pi r^4 Pt}{8l\eta} \qquad (11)$$

Relating the mercury flow rate to equation (11)

$$m = \frac{V\varrho}{t} = \frac{\pi r^4 \varrho P}{8l\eta} \qquad (12)$$

P can be expressed in terms of the mercury reservoir height corrected for the back pressure (i.e., the pressure opposing the capillary forces) as

$$P = g\varrho h \qquad (13)$$

From equation (12) and (13), it followsthat

$$m = \frac{\pi r^4 \varrho^2}{8l\eta} gh \qquad (14)$$

The weight of the drop at the end of its life time is gmt_{max}. This force is counterbalanced by the surface tension γ acting around the circumference of the capillary of radius r; thus

$$mgt_{max} = 2\pi r\gamma r \qquad (15)$$

From equations (12) and (15)

$$t_{max} = \frac{16\eta}{g(\rho r)^3 h} \qquad (16)$$

Thus equations (12) and (16) can be written as

$$m = k'h \qquad (17)$$

$$t_{max} = \frac{k''}{h} \qquad (18)$$

where k' and k'' are the constants of equation (12) and (16) respectively. Writing equation (8) in the form:

$$i_d = \text{Constant } m^{2/3} t^{1/6} \qquad (19)$$

and combining equation (19) with equations (17) and (18) we obtain the relationship:

$$i_d = \text{Constant } (k'h)^{2/3} \left(\frac{k''}{h}\right)^{1/6}$$

$$= \text{Constant } (k')^{2/3} (k'')^{1/6} h^{1/2} \qquad (20)$$

Hence the dependence of the limiting current on the

square root of the reservoir height can be used as a diagnostic criterion to distinguish diffusion controlled processes from other kinds of current limitation.

2.2. Kinetic Currents

For a polarographic limiting current which is controlled by the rate of prior chemical step, Koutecky's method (71, 72) permits one to establish the kinetics of the prior chemical reaction. This analysis is applicable to an electrode reaction scheme of the type:

$$A \underset{k_b}{\overset{k_f}{\rightleftharpoons}} O_x + ne \xrightarrow{} Red \qquad (21)$$

where O_x is reducible at a potential where A is not. However in some systems it is possible to reduce A directly at more negative potential than is needed to reduce O_x. The kinetic limiting current and the kinetics of the prior chemical step depend on both the ratio of the equilibrium concentrations of A and O_x in the bulk of the solution and the rate constants for their interconversion. We here discuss the pure kinetic current that is obtained when the equilibrium concentration of O_x is negligibly small, the transformation of A into O_x is very slow, and O_x is immediately reduced as soon as it reaches the electrode surface.

The original treatment of polarographic kinetic currents were developed by Brdicka and Wiesner (73, 74) on the assumption that the reaction controlling the current occurs in a reaction layer of somewhat arbitrary thickness. Koutecky and Bridicka (75) developed a rigorous treatment of kinetic currents for the case of linear diffusion. Koutecky (76) later transposed this treatment to the case of the DME by substituting a moving plane boundary for the expanding sphere. The results of this rather mathematically involved treatment is given by the equation:

$$i_k = nFDAC_A K^{1/2} K_f^{1/2} \qquad (22)$$

where $K = K_f / K_b$

Equation (22) can be written in the form:

$$i_k = k' A \qquad (23)$$

where $k' = nFDC_A K^{1/2} K_f^{1/2}$. Substituting equation (6) into equation (23)

$$i_k = k'' \, m^{2/3} t^{2/3} \qquad (24)$$

where $k'' = k' 4\pi \left(\frac{3}{4\pi}\right)^{2/3}$

Thus the log i - log t plot of the limiting current must be linear with a slope of 0.67. Since from equations (17)

and (18) m is directly proportional to the height of mercury and t is inversely proportional to the height of mercury, the kinetic current is independent of the height of mercury. These provide a simple test for distinguishing between a kinetically controlled and a diffusion controlled process.

The foregoing treatment is restricted to conditions under which the equilibrium concentration of O_x is very small while the concentration of A is constant throughout the solution. If however O_x exists in appreciable amounts the kinetic current will also include contributions resulting from its diffusion. The dependence of the log i log t, log i log h plots then will be intermediate between pure kinetic and pure diffusion controlled process.

2.3. Catalytic Currents

Catalytic processes arise from mechanisms of the the type:

$$O_x + ne \longrightarrow Red \qquad (25)$$

$$Red + Z \underset{K_b}{\overset{K_f}{\rightleftharpoons}} O_x$$

in which product being consumed in the electrochemical reaction is partially regenerated by a chemical process

involving a substance Z, which would not be reducible if it were present alone. Under the conditions that O_x is reduced as soon as it reaches the electrode surface, Z is present in a relatively very large excess, the rate of the backward reaction is negligible and $(K_f + K_b)C_z t$ is larger than 10, Koutecky (Ⱦ1, 77) derived the catalytic current over the life of a drop to be

$$i_c = nFAD_{ox}^{1/2} m^{2/3} t^{2/3} [(K_f + K_b)C_z]^{1/2} \qquad (26)$$

Thus the log i - log h and log i - log t plots behaviour for catalytic waves will be similar to those of kinetic currents, that is the currents are independent of the mercury reservoir height, and log i - log t plot will give slopes equal or greater than 0.67. The distinction between a catalytic and a kinetic current is the rapidity with which the chemical reaction takes place at the electrode surface.

Adsorption Currents

In the preceding discussions the distribution of a species was assumed to be the same throughout the solution, and double layer effects were neglacted. However, specific adsorption can occur at the electrode surface. This adsorption can involve an electroactive or electroinactive species, or, also, a substrate or a product.

The adsorption wave can be a prewave or a postwave to that of the reduction of the unadsorbed molecules or ions. Adsorption of the product of the reduction $O_x + ne \longrightarrow$ Red gives a prewave, because it is more difficult to reduce O_x to a dissolved Red than to reduce it to an adsorbed Red. At very low concentrations of O_x, there will be a single diffusion controlled prewave, until enough Red is formed to cover the whole mercury surface, beyond which a second wave begins to appear. If, on the other hand, O_x is adsorbed and Red is not, a single diffusion controlled wave is formed which is due to the reduction of adsorbed O_x, and which increases up to a certain depolarizer concentration. At higher O_x concentrations this wave is independent of concentration, but a second wave which increases with increasing concentration appears at a more negative potential.

In either of these cases the limiting current of the adsorption wave is proportional to the amount adsorbed on the drop during its life.

$$\text{moles of adsorbed species} = A\Gamma \qquad (27)$$

The charge consumed during the reversible reduction of an adsorbed depolarizer, is

$$q = nFA\Gamma \qquad (28)$$

The resulting instantaneous current is

$$i_a = \frac{dq}{dt} = nF \frac{d}{dt} (A\Gamma) \qquad (29)$$

Substituting equation (6) into (29)

$$i_a = nF\Gamma \frac{d}{dt} 4\pi \left[\frac{3mt}{4\pi\rho}\right]^{2/3} \qquad (30)$$

$$i_a = 0.57nF\Gamma m^{2/3}t^{-1/3} \qquad (31)$$

It follows from equations (17), (18) and (31) that $m^{2/3}t^{-1/3}$, and hence the limiting current of the adsorption current is proportional to the mercury reservoir height, and this is the fundamental criterion for adsorption controlled limiting current. Other diagnostic criteria include, the appearance of a new wave at a certain concentration of the depolarizer, and the decrease of the wave with increasing temperature. From equation (31) it is also clear that the current falls off with a $t^{-1/3}$ dependence. The adsorption of the depolarizer does not always cause the appearance of two waves. Sometimes only one wave is observed, but its shape is different from that of normal polarographic waves, since a large maximum is observed on the limiting portion of the wave.

2.5. Differential Pulse Polarography

In this technique a linearly increasing dc voltage is applied to the working electrode and a pulse of fixed height is super imposed on to this voltage.

The current is sampled just before the application of the pulse and near the end of the pulse, and the readout is the difference between the two currents giving a differential pulse polarogram (78, 79, 80).

Analytically, the chief advantage of differential pulse polarography (dpp) over conventional dc polarography is its ability to discriminate between faradaic and capacitative (charging) current. As a result it is very sensitive and enables the determination of metal ion concentrations down to at least 10^{-7}M for reversible electrode processes (78, 81, 82).

The form of the differential pulse polarography allows a more precise, determination of the peak potential as compared to the dc polarogram, where even the $E_{1/2}$ determined from the rather tedious E Vs $\log(\frac{id-i}{i})$ plot is not as precise (82, 83). The current sampling helps in getting a much less distorted polarographic wave than the dc technique. For a Nernestian system, the polarographic current - potential relation is

$$E = E_{1/2} - \frac{RT}{nF} \ln \frac{i}{id-i} \qquad (32)$$

Rearrangement of equation (32) gives

$$i = i_d \left(\frac{1}{1 + \exp (E-E_{1/2}) \frac{nF}{RT}} \right) \qquad (33)$$

Substituting the Cottrell expression, for i_d, and subsequent differentiation of equation (33) with respect to E yields

$$\Delta i = \frac{n^2F^2}{RT} AC \Delta E \left(\frac{D}{\pi t} \right)^{1/2} \frac{P}{(1 + P)^2} \qquad (34)$$

where $P = \exp (E - E_{1/2}) \frac{nF}{RT}$. Parry and Ostergoung (84) have shown that, for small pulse amplitudes (up to 50 millivolts), the maximum peak current is

$$i_p = \frac{n^2F^2}{4RT} AC \Delta E \left(\frac{D}{\pi t} \right)^{1/2} \qquad (35)$$

The peak half width, $W_{1/2}$ defined as the width of the peak in millivolts at the point where the peak current is one half its maximum height, is given from equations (34) and (35) to be

$$W_{1/2} = 3.52 \frac{RT}{nF} \qquad (36)$$

Equation (36) is normally used as a criterion of differential pulse polarographic reversibility. Parry and Osteryoug (84) have demonstrated that within

experimental errors, the peak potential is related to the half-wave potential by the expression:

$$E_p = E_{1/2} - \frac{\Delta E}{2} \qquad (37)$$

3. Cd(II) - Threonine System

3.1. Determination of Stability Constants by Polarography

The polarographic method for the determination of the stability constants of complexes is in general based on the shift of half-wave potentials. The method was first developed by Lingane (1) and is applicable to systems involving essentially one very stable complex. Later, Deford and Hume (2) developed a method for the case of successive complex formation based on determining the dependence of the half-wave potential of the diffusion controlled wave of reversible metal reduction on the complex forming agent concentration. Since these two methods are the basis for the present investigation, their derivations is reproduced below. Several cases have been treated in the literature, namely the case where the ligand concentration is not in excess (3, 4, 5), where the electrode reeuction is irreversible but where the ligand is in excess (5,6) or where the ligand is not in excess (5). Schaap and Mc masters (7) have also extended the Deford - Hume method to the case of mixed ligand complexes. However these latter cases have not been studied in the present work and therefore will not be treated here. Stability constant determination for reversible cases will now be presented.

3.1. 1. Single - complex formation. (The Lingane Method) when only one complex is formed, the reversible

reduction of a complex of a metal soluble in mercury can be represented as

$$MX_p^{+(n-pb)} + ne \rightleftharpoons M(Hg) + pX^{-b} \qquad (1)$$

This reaction can be regarded as

$$MX_p^{+(n-pb)} \rightleftharpoons M^{+n} + pX^{-b} \qquad (2)$$

and $$M^{+n} + ne + Hg \rightleftharpoons M(Hg) \qquad (3)$$

The formation constant β for equilibrium (2) is

$$\beta = \frac{C^o_{mx_p} f_{mx_p}}{C^o_m f_m (C^o_x f_x)^p} \qquad (4)$$

For a diffusion controlled process

$$i = k_c(C_{mx_p} - C^o_{mx_p}) \qquad (5)$$

and $$i_d = k_c C_{mx_p} \qquad (6)$$

where $$k_c = 706\ n\ D^{1/2}_m 2/3 t^{1/6} \qquad (7)$$

Under the condition where a relatively large excess of ligand exists, i.e, when the ligand concentration can be assumed to be virtually a constant, then use of equations (5) and (6) in the Nernst equation gives

$$E = E^o - \frac{RT}{nF} \ln \frac{\beta f Red}{f_{mx_p}} \left(\frac{D_{mx_p}}{D_m}\right)^{1/2} - \frac{RT}{nF} \ln \frac{i}{i_d - i} (C^o_x f_x)^p \qquad (8)$$

which can be rewritten as

$$E = (E_{1/2})_c + \frac{RT}{nF} \ln \frac{i_d - i}{i} \qquad (9)$$

where $(E_{1/2})_c = E^o - \frac{RT}{nF} \ln \frac{\beta Red}{f_{mx_p}} \left(\frac{D_{mx_p}}{D_m}\right)^{1/2}$

$$- p \frac{RT}{nF} \ln C_x^o f_x \qquad (10)$$

From equation (9) it follows that

$$(E_{1/2})_c - (E_{1/2})_M = - \frac{RT}{nF} \ln \frac{\beta f_m}{f_{mx_p}} \left(\frac{D_{mx_p}}{D_m} \right)^{1/2}$$

$$- p \frac{RT}{nF} \ln C_x^o f_x \qquad (11)$$

Equation (10) enables the determination of the ligand number p through a plot of $E_{1/2}$ versus $\ln C_x$. Use of the p value in equation (11) yields β, provided both D_m and D_{mx_p} are known. In most cases their difference is so small that they are taken to be equal. The calculations often are even more simplified by assuming activity coefficients of unity.

2. Formation of a series of complexes with a single ligand (The Deford-Hume method).

In this category, there are two classes of systems, viz,

i. those in which each complex exists only within a definite region of ligand concentration, and

ii. systems which consist of a series of complexes in step - equilibria.

Occassionally, a plot of log C_x against $(E_{1/2})_c$ produces a segmented curve, indicating the presence of a series of complexes whose stability constants and formulae may be found from the various segments using the Lingane's method.

For systems involving a series of complexes of comparable stability and which maintain fast equilibria, defining the step - wise overall stability constant K_j for

$$M^{+n} + jx \;\text{====}\; MX_j \qquad (12)$$

$$\text{as } K_j = \frac{C_{mx_j} f_{mx_j}}{(C_x f_x)^j C_m f_m} \qquad (13)$$

then

$$C_m^o f_m = \frac{\sum_{j=o}^{N} C_{mxj}^o}{\sum_{j=o}^{N} \frac{K_j (C_x f_x)^j}{f_{mx_j}}} \qquad (14)$$

If the reduction is diffusion controlled, then an extension of the above treatment yields

$$E = E^o - \frac{RT}{nF} \ln \left[\frac{D_c}{D_m}\right]^{1/2} \cdot \sum_{j=o}^{N} \frac{K_j}{f_{mx_j}} -$$

$$- \frac{RT}{nF} \ln (C_x f_x)^j - \frac{RT}{nF} \ln \frac{i}{id-i} \qquad (15)$$

Leting $(E_{1/2})_c = E^o - \frac{RT}{nF} \ln \left(\frac{Dc}{D_m}\right)^{1/2} \sum_{j=o}^{N} \frac{K_j}{f_{mx_j}} -$

$$- \frac{RT}{nF} \ln (C_x f_x)^j \qquad (16)$$

then, $(E_{1/2})_m - (E_{1/2})_c = \frac{RT}{nF} \ln \left(\frac{Dc}{Dm}\right)^{1/2} \sum_{j=o}^{N} \frac{K_j}{f_{mx_j}} +$

$$+ \frac{RT}{nF} \ln (C_x f_x)^j \qquad (17)$$

From equation (17), it follows that

$$\text{antilog}\left[\frac{nF}{2.303RT} \left[(E_{1/2})_m - (E_{1/2})_c \right] + \log \left(\frac{Dc}{Dm}\right)^{1/2}\right] = \sum_{j=o}^{N} \frac{K_j (C_x f_x)^j}{f_{mx_j}} \qquad (18)$$

$$C_m^o f_m = \frac{\sum_{j=o}^{N} C_{mxj}^o}{\sum_{j=o}^{N} \frac{K_j (C_x f_x)^j}{f_{mx_j}}} \qquad (14)$$

If the reduction is diffusion controlled, then an extension of the above treatment yields

$$E = E^o - \frac{RT}{nF} \ln \left[\frac{D_c}{D_m}\right]^{1/2} \cdot \sum_{j=o}^{N} \frac{K_j}{f_{mx_j}} -$$

$$- \frac{RT}{nF} \ln (C_x f_x)^j - \frac{RT}{nF} \ln \frac{i}{id-i} \qquad (15)$$

Leting $(E_{1/2})_c = E^o - \frac{RT}{nF} \ln \left(\frac{Dc}{D_m}\right)^{1/2} \sum_{j=o}^{N} \frac{K_j}{f_{mx_j}} -$

$$- \frac{RT}{nF} \ln (C_x f_x)^j \qquad (16)$$

then, $(E_{1/2})_m - (E_{1/2})_c = \frac{RT}{nF} \ln \left(\frac{Dc}{Dm}\right)^{1/2} \sum_{j=o}^{N} \frac{K_j}{f_{mx_j}} +$

$$+ \frac{RT}{nF} \ln (C_x f_x)^j \qquad (17)$$

From equation (17), it follows that

$$\text{antilog}\left[\frac{nF}{2.303RT} \cdot \left[(E_{1/2})_m - (E_{1/2})_c \right] + \log \left(\frac{Dc}{Dm}\right)^{1/2}\right] = \sum_{j=o}^{N} \frac{K_j (C_x f_x)^j}{f_{mx_j}} \qquad (18)$$

Leden's graphical method is then used to evaluate the stepwise overall stability constants, i.e.

$$\text{if antilog}\left\{\frac{nF}{2.303RT}[(E_{1/2})_m - (E_{1/2})_c] + 1/2 \log \frac{Dc}{Dm}\right\} = F_{o(x)} \qquad (19)$$

$$\text{then } F_o(x) = \frac{K_o}{f_m} + \frac{K_1 C_x f_x}{f_{mx}} + \ldots + \frac{Kn(Cxfx)^n}{f_{mx_n}} \qquad (20)$$

If $F_1(x)$ is now defined as:

$$\frac{Fo(x) - \frac{Ko}{f_m}}{C_x f_x} = F_1(x) \qquad (21)$$

$$\text{then } F_1(x) = \frac{K_1}{f_{mx}} + \frac{K_2 C_x f_x}{f_{mx_2}} + \ldots + \frac{K_n (C_x f_x)^{n-1}}{f_{mx_n}} \qquad (22)$$

Sullivard and Hindman (8) have shown that

$$\lim_{C_x f_x \to o} \frac{Fo(x) - \frac{Ko}{fm}}{C_x f_x}$$ is not an indeterminate

form but is equal to K_1, the first step stability constant, since

$$\lim_{C_x f_x \to o} \frac{Fo(x) - \frac{Ko}{fm}}{C_x f_x} = \lim_{C_x f_x \to o} \frac{\partial(Fo(x) - \frac{Ko}{fm})}{\partial C_x f_x} \qquad (23)$$

$$= \lim_{C_x f_x \to 0} K_1 + 2K_2\, C_x f_x + \ldots + nK_n (C_x f_x)^{n-1}$$

$$= K_1$$

similarly $$\lim_{C_x f_x \to} \frac{F_1(x) - K_1}{C_x f_x} = K_2 \qquad (24)$$

It follows from equation (22) that the curve of $F_1(x)$ against $C_x f_x$ gives the value of K_1 on the formation axis. then the next function, $\frac{F_1(x) - K_1}{C_x f_x}$, against $C_x f_x$ gives K_2 as an intercept. Continued treatments will give a straight line parallel to the concentration axis of the ligand, for the highest coordination number. A similar plot for the immediately preceding complex will be a straight line with a positive slope and all previous function plots will show curvature.

3.2. Effect of pH on Complexation

In all the calculations so far mentioned the effective ligand concentration has to be used in the concentration terms. Most ligands, being fairly basic, get easily protonated. Therefore the free ligand concentration available for complexation has to be calculated. The

total ligand concentration is equal to the sum of the ligands coordinated to the metal, plus that which is free, plus that which is protonated. In the form of an equation

$$[X] = C_m \sum_{j=i}^{N} j\beta j(C_x)^j + C_x\alpha_{(H)} \qquad (25)$$

where $\alpha_{(H)} = \frac{[X]}{C_x}$ (26)

If the ligand is in a fairly large excess over the metal ion concentration as is particularly true in this case, then

$$[X] = C_x\alpha_{(H)}$$

But $[X] = C_x + C_x [H] K_1^1 + C_x[H]^2 K_1^1 K_2^1 + \ldots$ (27)

Hence $\alpha_{(H)} = 1 + [H] K_1^1 + [H]^2 K_1^1 K_2^1 + \ldots$ (28)

Combination of (26) and (28) gives the free ligand concentration C_x from known values of pH, and the successive protonation constants of the ligand.

3.3. Experimental

The chemicals used, Na_2HPO_4, H_3BO_3, $Na_2B_4O_7$, $CdSO_4$ and chromatographically homogeneous threonine, BDH, were all of reagent grade purity. All polarograms were done at 10^{-4}M $CdSO_4$ and 0.06M $Na_2B_4O_7$ (pH 9.2) unless otherwise stated. Any increase in the metal concentration above 10^{-4} molar resulted in precipitation at this pH. Measurements were taken under thermostatic conditions at (25 ± 0.5)°C using a precision Scientific Instruments heating pump (model 66590). Polarograms were obtained using the Metrohm Polarecord E506, and the rapid polarographic technique with a droptime of 3 seconds was achieved with a Metrohm polarographic stand E505. A scan rate of 1 milli-volt per 3 seconds was used. All solutions were flushed with nitrogen for 10 minutes and then kept under an atmosphere of nitrogen while recording the polarograms. The mercury reservoir height was kept constant at 57 cms. pH measurements were taken using a Beckman Chem-Mate pH meter. All potential measurements were taken against the Ag/AgCl, KCl (sat'd) reference electrode.

3.4. Results and Discussion

In order to study the cadmium - threonine polarographic behaviour, the pH in which threonine can complex, as well as a suitable buffer had to be chosen.

Among the usual inorganic buffers of relatively high pH and ones which do not interfere as competing ligands, borate and phosphate buffers were selected. The diffusion current recorded for 10^{-4}M $CdSO_4$ in 0.06M Na_2HPO_4, pH 9.3, was eleven times less than that in 0.06M $Na_2B_4O_7$, pH 9.2, supporting electrolyte, under otherwise exactly the same conditions. Besides, well defined waves without any maxima were obtained in the borate buffer. Therefore all studies were carried out in this media.

3.4.1. Effect of pH

The effect of pH on the electroreduction of the complex had to be considered in view of the fact that there is competition between the proton and the metal for the ligand. Polarograms were taken for solutions that were 10^{-4}M $CdSO_4$, 2.5 x 10^{-3}M threonine, 0.06M $Na_2B_4O_7$ but varying concentration of H_3BO_3, thereby effecting a change in pH. The addition of boric acid did not show any change on the magnitude of the diffusion current. With raising pH the half - wave potentials shifted toward more cathodic potentials (table 1, Figure 1). This shift toward more negative potentials is due to the increase in the free ligand concentration as shown in Figure 2. In addition the pH dependence indicated that in the range coonsidered,

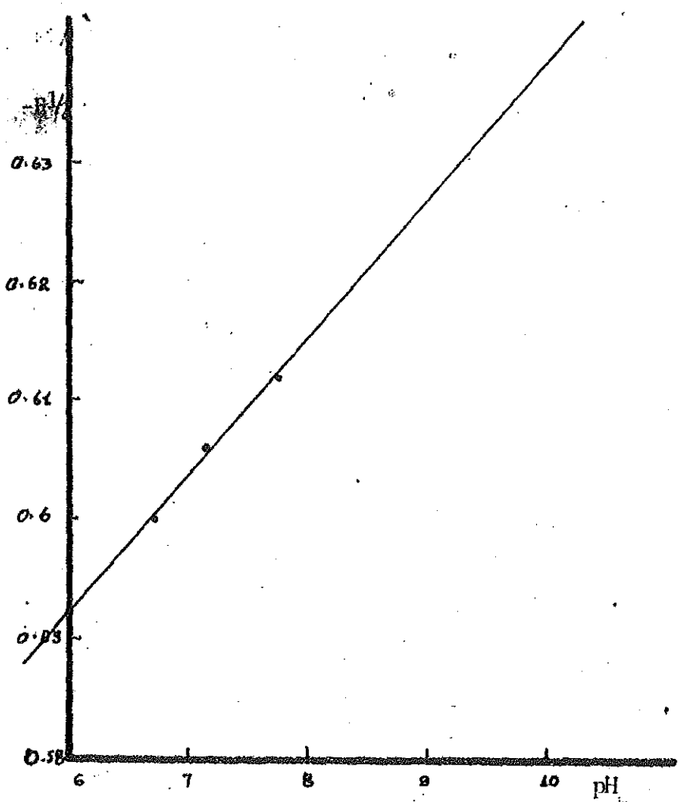

Figure 1. Plot showing the $E_{1/2}$ dependence on pH for 0.1mM Cd(11), 2.5mM threonine in 0.06m borax and varying conc. of boric acid.

$[H_3BO_3]$ M	pH	$-E_{1/2}$	[Threonine] M	-log [thr$^-$]
Saturated	6	0.592	2.33×10^{-6}	5.63
0.8	7.7	0.6	1.163×10^{-5}	4.93
0.6	7.15	0.606	3.251×10^{-5}	4.49
0.4	7.75	0.612	1.25×10^{-4}	3.9
0.2	8.4	0.620	4.75×10^{-4}	3.32
0.1	8.7	0.636	7.97×10^{-4}	3.1
-	9.2	0.639	1.49×10^{-3}	2.83

Table 1: $-E_{1/2}$ values for varying pH, for solutions of 10^{-4}M $CdSO_4$, 2.5×10^{-3}M threonine, 0.06M $Na_2B_4O_4$ and varying H_3BO_3 concentrations.

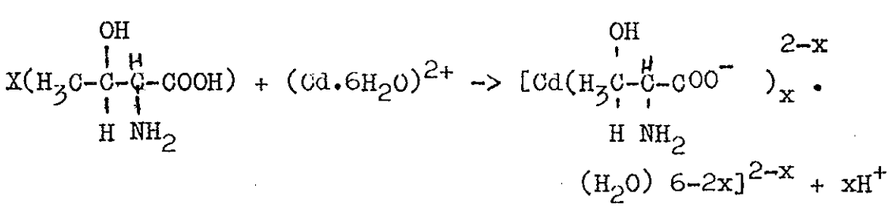

is not complete. Hence one cannot take the analytical threonine concentration as the free ligand concentration. Indeed the analytical concentration is about equal to the free ligand concentration only when the pH is greater than or equal to pKa + 2. Since a maximum half-wave potential shift was obtained in 0.06M $Na_2B_4O_7$, the effect of threonine concentration was studied in this media.

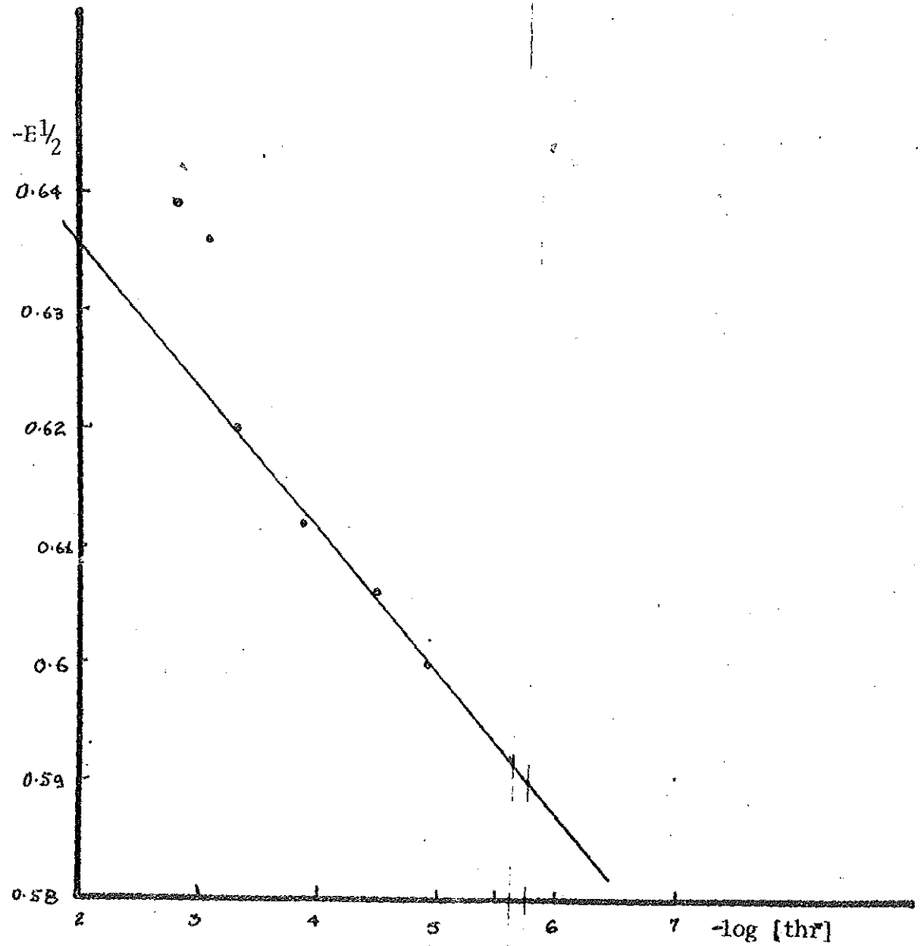

Figure 2. Plot showing the dependence of the $E_{1/2}$ on threoninate conc. for 0.1mM Cd(11), 2.5mM threonine, 0.06m borax and varying boric acid conc.

3.4.2. Effect of Varying Threonine Concentration

The effect of increasing threonine concentration over a range form 7.45×10^{-4}M to 11.933×10^{-3}M of threoninate on the polarograms of 10^{-4}M $CdSO_4$ in 0.06M $Na_2B_4O_7$ showed half-wave potential shifts toward more negative potentials with increasing threoninate concentration Fig. (3). The reduction of cadmium both as a simple metal ion and as acomplexed metal ion is reversible as shown by E vs log $\frac{i}{i_d - i}$ plots shown in Figure 4. This plot gave a slope of 30 milliwolts for the simple metal ion only, and 31 millivolts for a representative polarogram of the complex that is 10.442×10^{-3}M in threoninate. Therefore this system is amenable to the Deford-Hume method of stability constant determination. In table 2 is given the experimentally determined half-wave potentials with the calculated values of $Fo(x)$, $F_1(x)$, and $F_2(x)$ which are also plotted in Figures, 5, 6 and 7 respectively.

[Threoninate] in molarity	$E_{1/2}$ in V	$F_{o(x)}$	$F_{1(x)}$	$F_{2(x)}$
	-0.614	1.00	-	-
7.458×10^{-4}	-0.624	2.178	1.58×10^{3}	0.44×10^{6}
2.983×10^{-3}	-0.642	8.842	2.63×10^{3}	0.46×10^{6}
5.967×10^{-3}	-0.6544	23.214	3.72×10^{3}	0.41×10^{6}
8.95×10^{-3}	-0.664	49.001	5.36×10^{3}	0.46×10^{6}
10.442×10^{-3}	-0.667	61.903	5.83×10^{3}	0.51×10^{6}
11.933×10^{-3}	-0.6706	81.925	6.78×10^{3}	0.46×10^{6}

Table 2: Table of the $F_{(x)}$ functions. System: 10^{-4} in $CdSO_4$, 0.06M $Na_2B_4O_7$ - and varying concentrations of threoninat

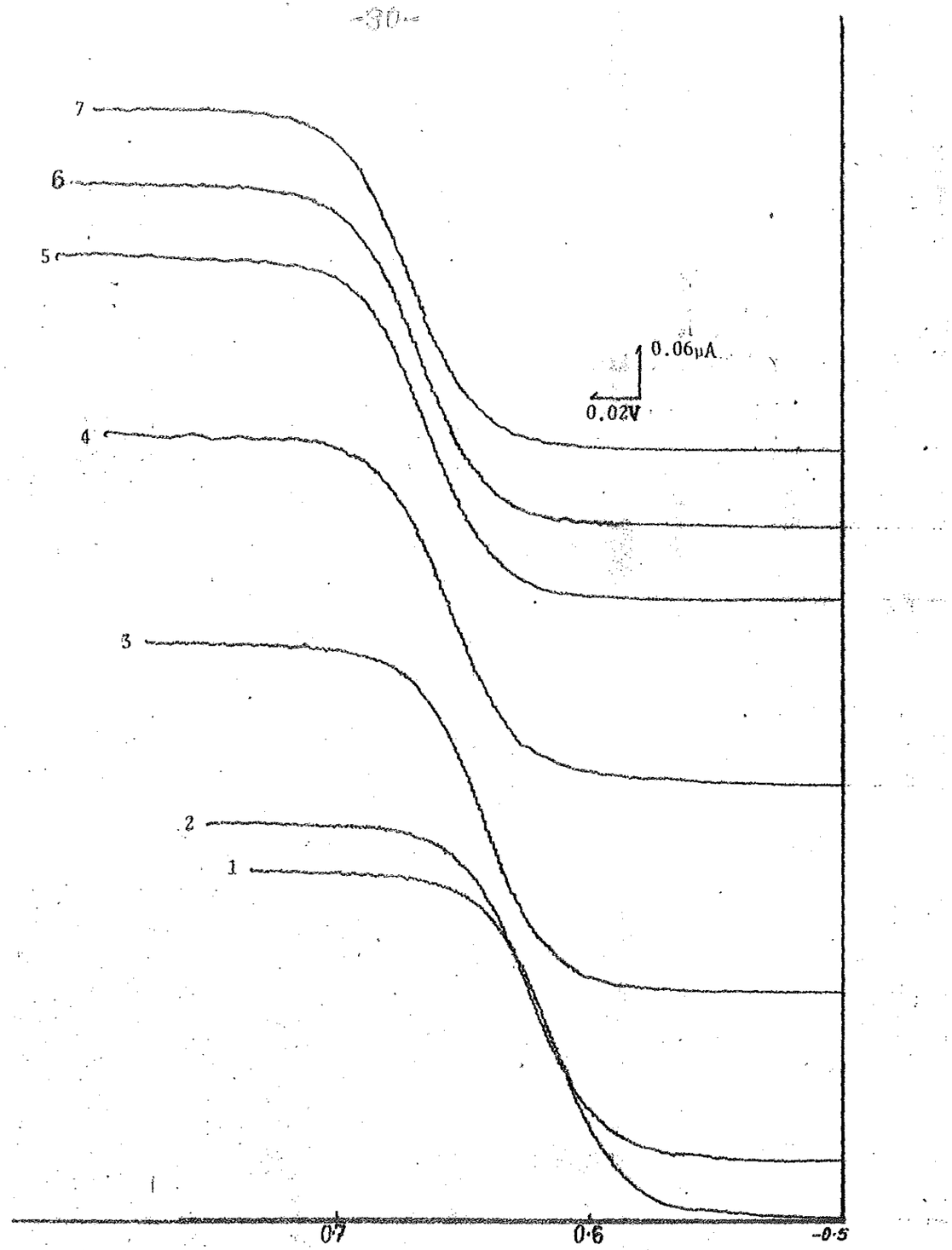

Figure 3. Polarograms of 0.1mM Cd(11), 0.06m borax. threonine conc., 1,0; 2,7.45(
2.983; 4, 5.967; 5, 8.95; 6, 10.442; 7, 11.933; mM. Commencing potent

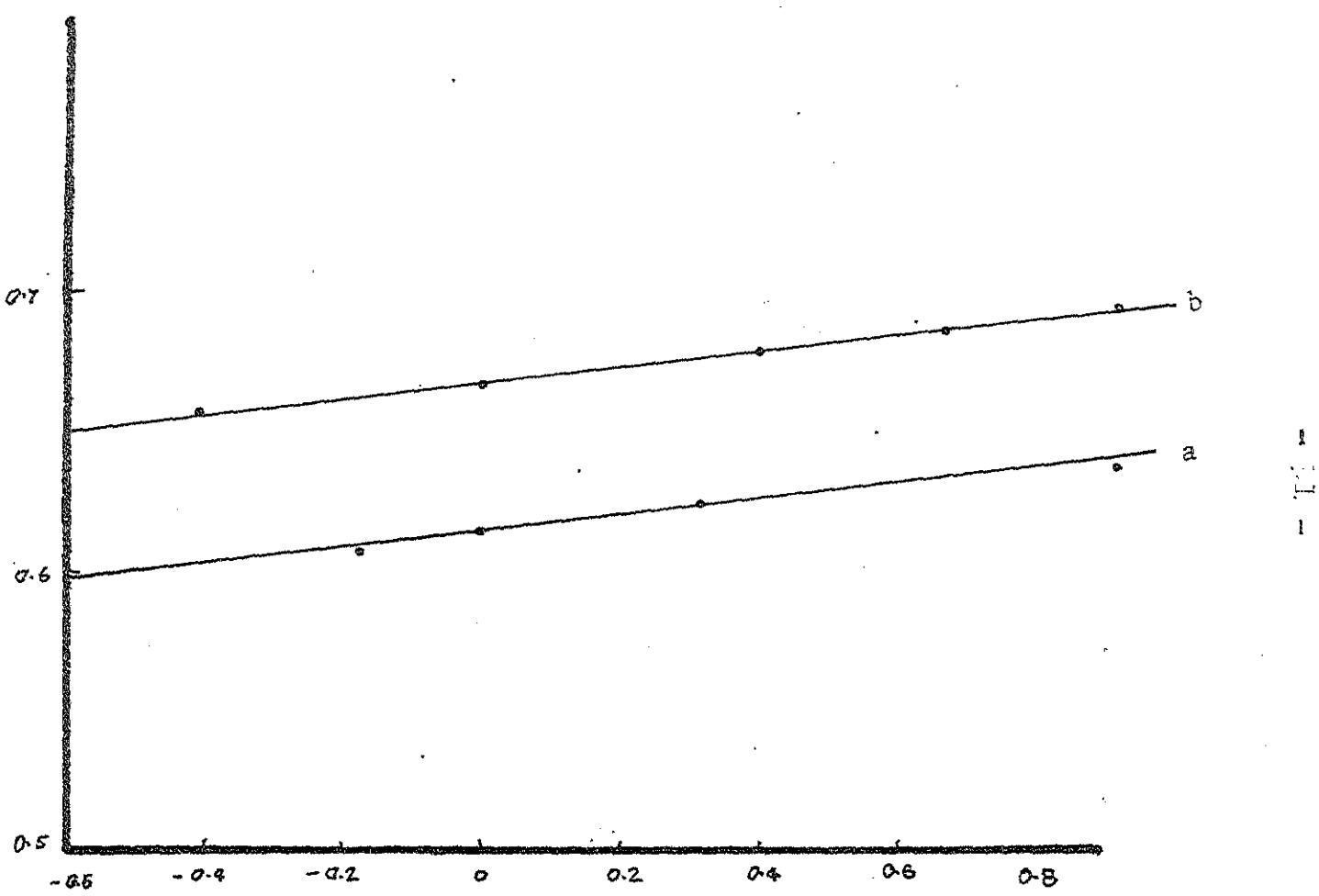

Figure.4. Plot of E Vs log $\frac{i}{i_{d-i}}$ for 0.1mM Cd(II), 0.06m borax, threonine conc., a,O; b, 10.-42mM.

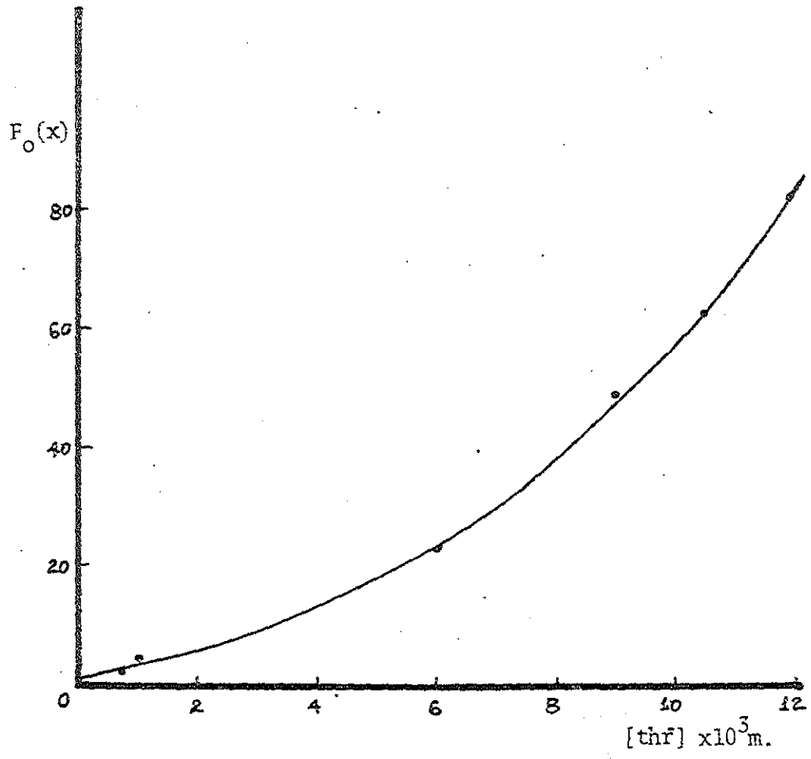

Figure 5. Plot of $F_o(x)$ Vs threoninate conc.

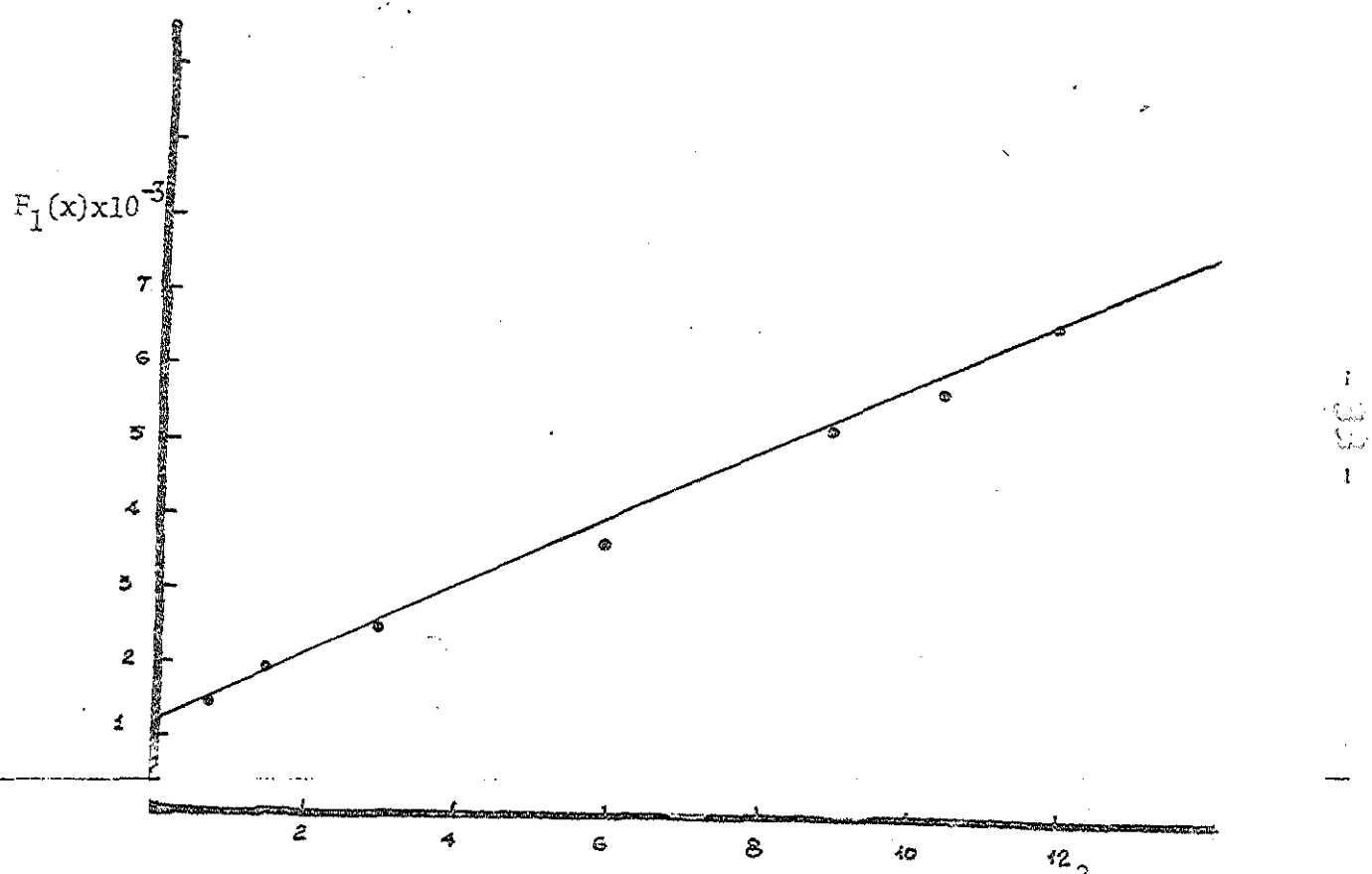

Figure 6. Plot of $F_1(x)$ Vs threonine conc.

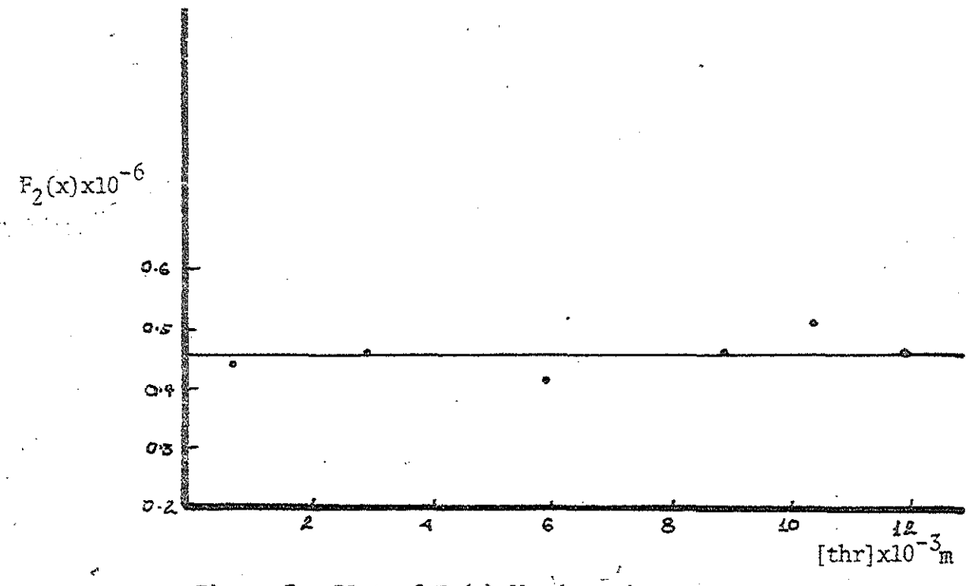

Figure 7. Plot of $F_2(x)$ Vs threonine conc.

As is evident from equation (22), $F_{i(x)}$ can only be linear, as shown in Figure 6, provided it has the following form

$$F_{1(x)} = K_1 + K_2 C_x$$

The intercept of $F_{1(x)}$ versus threoninate concentration therefore must yield the K_1 value and its slope must equal the second overall stability constant. These have been determined to be $K_1 = 1.25 \times 10^3$ ($\log K_1 = 3.1$) and $K_2 = 4.6 \times 10^5$ or $\log K_2 = 5.67$. The K_2 value is further confirmed by the $F_{2(x)}$ dependence on the threoninate concentration which gave an identical value as is shown in Figure 7. Hence $\log k_2 = 2.57$.

Conclusion

The reduction of cadmium on the dropping mercury electrode both as a complex of threonine and simple metal ion is reversible in borate buffer. The complexation has been found to be pH dependent and the stability constants calculated with this into account. The stepwise stability constants calculated using the Deford-Hume method are $\log K_1 = 3.1$ and $\log k_2 = 2.57$.

4. Cobalt and Nickel - Threonine Systems

4.1. Polarographic Behaviour of Co(II) and Ni(II) Complexes

The polarographic behaviour of Ni(II) and Co(II) have been studied by several workers, in different media and also with different complexing agents. Many of these studies have been initiated because their behavior strongly depended on the nature of the ligands involved and the structures of the complexes formed. Positive shift in the half-wave reduction potentials, double wave formation and enhanced current magnitudes for the prewave, are among the prominent features of these metal reductions. The following postulates have been forwa ded to explain the mechanism of these reductions.

1. Adsorption of the ligand on the mercury surface:- Many anions and neutral organic compounds get specifically adsorbed on mercury. This adsorption has too often lead to the occurrence of a prewave at potentials more positive than that corresponding to the normal reduction potential (11, 12). The decrease in the reduction potential of complexed cations is due to the strong polarization of the complex owing to the formation of a bond with the adsorbed reactant and to the influence of the electric field in the interface between the catalyst and the solution. The activation energy of

this process is much decreased by such polarization, the complex being much more reactive in the adsorbed state (11). Thus adsorption can lead to the possibility of splitting of a reduction wave due to a single kind of depolarizer (13), a first wave resulting at the potential of adsorption, and a second one resulting at more negative potentials in which the reduction product of the first wave is desorbed.

Adsorption prewaves have been observed for complexes of Ni(II) and Co(II) with capillary active substances. Usually these prewaves are also catalytic, since the cyclic regeneration of the adsorbed ligand results in a higher flux of the metal ion Ni(II) complexes of phenylenediamine (14), pyridine (15) thiourea (16), thiocyanate ions (17) seleno-cysteine (18) and other amines (19) exhibit waves which have been attributed to a mechanism involving an adsorbed species (20). Co(II) waves with seleno-cystein (18) and several cystein like compounds (21) also give similar prewaves resulting from the same kind of mechanism as for adsorbed ligand Ni(II) complexes.

2. Desolvation controlled Reduction

In aqueous solution, transition metal ions are surrounded by a coordination sheath consisting

usually of six nearly-octahedrally arranged water molecules. The discharge of such an ion will be preceded by a step in which the coordination shell is rearranged in order to allow the ion access to the metal surface. However, such processes are not normally observed to be rate determining.

The ligand field theory has been successfuly used for the qualitative interpretation of the kinetic stability of complex compounds. As this has major influences on the electrode reduction mechanism and kinetics, it is essential to discuss it at length. The electronic configurations with the most important crystal field stabilization energies for metal complexes of ocrahedral micro-symmetry, which will show the highest kinetic stability are, d^3, d^6 (low-spin) and d^8. Aside from the crystal field stabilization energies, mutual interactions between the metal outer orbital d electrons and the ligands contribute to the kinetic stability. In the divalent ion series, Ni^{2+} has the d^8 configuration. Therefore one would expect its discharge to be not a simple diffusion controlled process, but principally controlled by a kinetic one. This includes both the hydrated and complexed octa-hedral Ni(II) reductions. Many studies show that the introduction of a foreign ligand into the inner

coordination sphere of Co(II) and Ni(II) aquo ions play a role in the kinetics of exchange and lability of the coordinated water molecules. Two types of rates are observed by two groups of ligands. The first group contains simple ligands such as ammonia, chloride, thiocynate ions, in fact ligands in which δ-bonding between ligand and cation is of predominant importance. Replacement of coordinated water by ligands in this group results in greater ease of displacement of the remaining water molecules, as a result of the reduction of the effective charge on the metal. The remaining metal (11) to water bonds will thereby be weakened.

The second group of ligands which include diamines of the bipyridyl and phenanothroline type, have little effect on rates of water exchange for the remaining coordinated water molecules. The effect of the δ-election donation by the ligand is counterbalanced through π - backbonding from the metal. In consequence the effective charge on the central metal atom is not altered. Thus, the metal water bonds remain as strong as those in the hexa - aquo - complex and the rate of water exchange is little affected.

Another kinetic step can be involved in the complexation of polydentate ligands with aquo cations. Such complexations take place in the following way

$$M(H_2O)_6^{2+} + L - L \underset{k_{d_1}}{\overset{k_s}{\rightleftharpoons}} M(H_2O)_5\,(L\text{-}L)^{2+} + H_2O$$

$$M(H_2O)_5(L\text{-}L)^{2+} \underset{k_{d_2}}{\overset{k_{ch}}{\rightleftharpoons}} M(H_2O)_4 \left(\begin{array}{c} L \\ | \\ L \end{array}\right)^{2+} + H_2O$$

where the ks refer to rates of dissociation (k_{d_1}, and k_{d_2}), substitution (k_s) and chelation (k_{ch}). If $k_{ch} >> k_{d_n}$ and k_s then the same kinetic pattern will be observed as for reaction with a monodentate ligand. If however, k_{ch} is about equal or is less than k_{d_1} and k_s, then the overall rate is controlled by chelation and is known as sterically controlled substitution. This step has been proved to be rate limiting for Co(II) aquo chelation with several bidentates (22). Because rates of solvents loss from Ni(II) are slow, rates of ring closure are rarely kinetic controlling. The difficulty attendent on closing the ring makes chelation, rather than water loss aquo-Co(II), rate limiting. Although no systenatic conclusions have been made for charged polydentate ligands, it is reasonable to expect both factors, namely ligand - assisted labilization and ring closure, must operate.

The effect of ligand - assisted labilization on the polarography of the cations is a decrease in the overvoltage of the reduction potential. If the labile and non-labil species simultaneously exist in solution a double wave can result. Many polarographic works have been reported in which such decrease in the reduction potential is accounted for by the desolvation process of Ni(II) and Co(II). Ni(II) forms two kinetic steps with glycine (23).

Spectroscopic studies (24) have confirmed that this results from the release of water. Several such kinetic Ni(II) complex reductions have been observed with pyridine (15), O - phenylenediamine (14) acetylacetonate (25) selenocysteine (28), citrate, tartarate (26) and chloride complexes (27). The work of Connick and Coppel (28) also support that the introduction of a foreign ligand increases the water - ligand exchange. Likewise, Co(II) complexes are also believed to show kinetic controlled reductions. The catalytic prewaves of Co(II) with dimethyldithiocarbamate (29), acetylacetonate (30, 31) selenocysteine (18), cysteine (21), and similar other compounds (32, 33), all are believed to arise from the relatively slow dehydration step. This effect is also observed in solvents. The easier the desolvation, the more reversible is the reduction, pink alcoholated $Co(MeOH)_n^{2+}$ (34), Ni(II) in DMF (35) and in weaker base solvents (36, 37) than water are more reversibly reduced, in contradistinetion to the irreversible reduction in water. Although the study of Eriksrud (38) concludes the possible slow dehydration step as unlikely in the rate control, most works employing other techniques (39, 40, 41, 42) have proved water-exchange of Co(II) and Ni(II) complexes to be kinetic steps.

3. Formation of an easily reducible complex.

Both Co(II) and Ni(II) reduction half-wave potentials are shifted to more positive values in the presence of large concentrations of chloride ions (43, 44, 27, 45, 46). It is postulated that there is the formation of a chloride complex which is more easily reduced than the aquated cation. In particular nickel forms tetrahedral $NiCl_4^{2-}$ (47, 48) whose orbital is may be more closely analogous to that of the actiuated reduction intermediate resulting in a lower activation energy (27). The positive shift of methyl red complex of nickel (49) has been attributed to the formation of an easily reducible complex. Zothi and Filloni (50) emphasize that Nickel, having a large π - bonding ability requires empty π - orbitals on the ligand for π - back bonding, which will lower the activation barrier for the election transfer. On the whole it is believed that the resulting change in the orbital configuration is responsible for the decrease in the activation overpotential.

4. The ligand serving as a bridge which facilitates the electron transfer.

The reduction potential of several cations has been observed to shift progressively towards

more positive potential with increasing number of double bonds of solvents (51, 52, 53). According to these authors, this is solely not a result of lower solvation energy but is due to the presence of conjugated double bond system on the solvation sphere of the metal, as well on the electrode which serve as a bridge for the electron transfer.

The separation into the above four major mechanisms is based only on degree of emphasis. Infact, although it may be difficult to tell the extent of influence of one kind of mechanism over the other in a certain reduction, at times more than one of the mechanisms can be involved.

4.2. Experimental

In the study of the polarographic behaviour of Co(II) and Ni(II), threonine complexes, the same instrument as that used in the study of the Cd(II) - threonine system was employed. However, since differential pulse polarography is more sensitive and gives better resolved peaks than DC polarography, this technique was mainly used in this work, except in the examination of the droptime and mercury reservior hight dependences of the limiting current, in which case DC polarography was employed. A pulse amplitude of 50 millivolts, a droptime of 3 seconds and a mercury reservior height of 57 cms. was maintained in all the experiments, except for the Ni(II) data of Tables (1) and (2) which were done at a mercury reservior height of 47 cms and a droptime of 2 seconds. Unless otherwise stated the voltage scan were commenced at -0.8V (all potentials reported in this work are relative to the Ag/AgCl/ (kcl saturated) reference electrode) and a scan rate of 2 millivolts per 3 seconds was used. All measurements were made at 25 $\pm$ 0.5°C and solutions were daerated with nitrogen, and the solutions blanketed with nitrogen throughout the measurement. All reagents used were of reagent grade purity.

4.3. Results of Co(II)-Thereonine System

Following the work of kolthoff and Mader (54) in which the polarographic reduction of cobalt in 0.06M borax buffer was reported, the present investigation of the polarographic behaviour of the cobalt - threonine system was undertaken also in the same supporting electrolyte. The effect of pH, metal and ligand concentrations were investigated and the results are reported below.

4.3.1. Effect of Threonine Concentration

The effect of threonine concentration in the range 5×10^{-5}M to 10^{-3}M on the Co(II) - threonine reduction was studied in 0.06M borax, and for three different constant concentrations of Co(II), viz, 10^{-4}M, 3×10^{-4}M and 4×10^{-4}M solutions. The values of the peak current and potential are given in tables (1), (2) and (3). The peak potential of the simple metal ion is -1.29v in 0.06M borax. Addition of threonine shifts the peak potential towards a more positive potential upto about -1.23v. The peak current increases and then levels off with increasing threonine concentration (see Figure (1)). The peak current of the complex is more tha 2.5 times that of the simple metal ion when the solution is 10^{-3}M

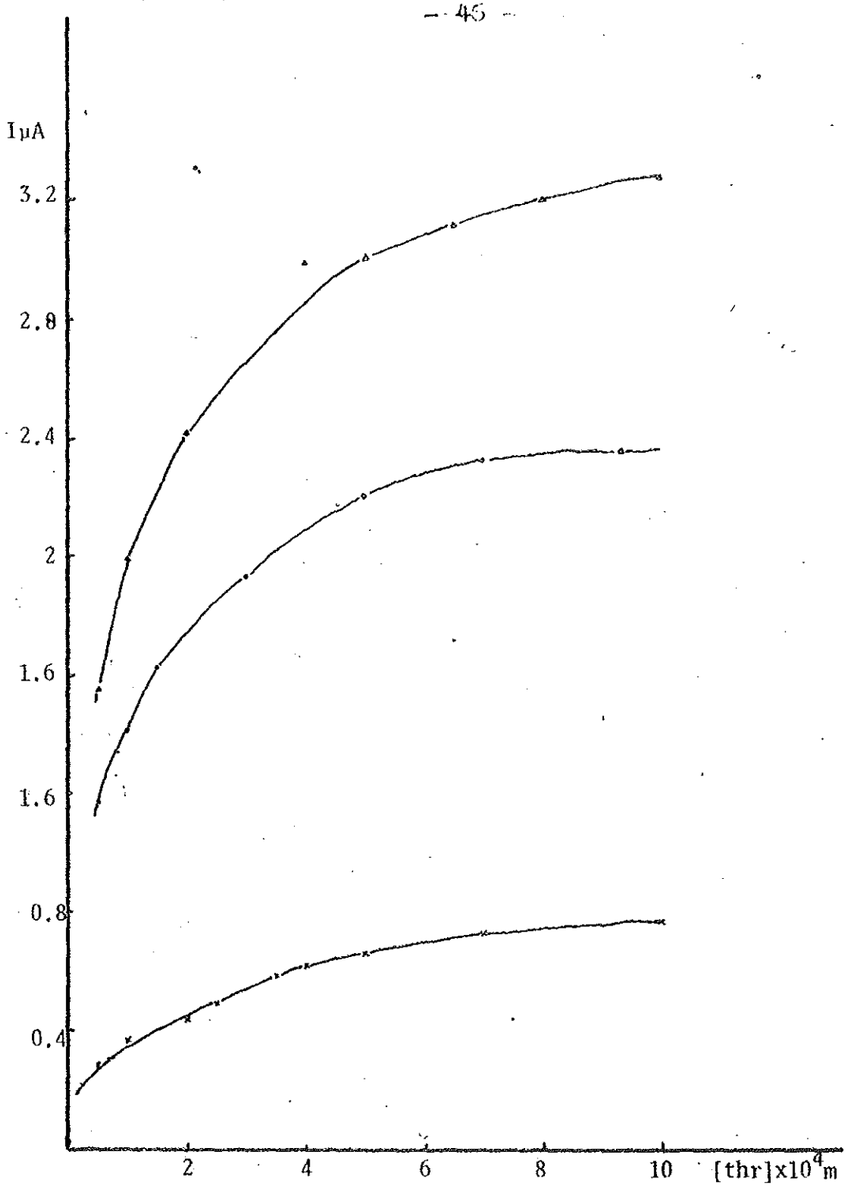

Figure 1. Plot of peak current Vs. threonine conc. in 0.06m borax. Co(11), 0.1(x), 0.3(o) and 0.4(∇)mM.

Figure 2. Polarograms showing effect of threonine. 0.3mM Co(II), 0.06M borax, Conc. of threonine 1, 0; 2, 0.05; 3, 0.15; 4, 0.3; 5, 0.5; 6, 0.75; 7, 0.994; 8, 2.25; 9, 15; mM.

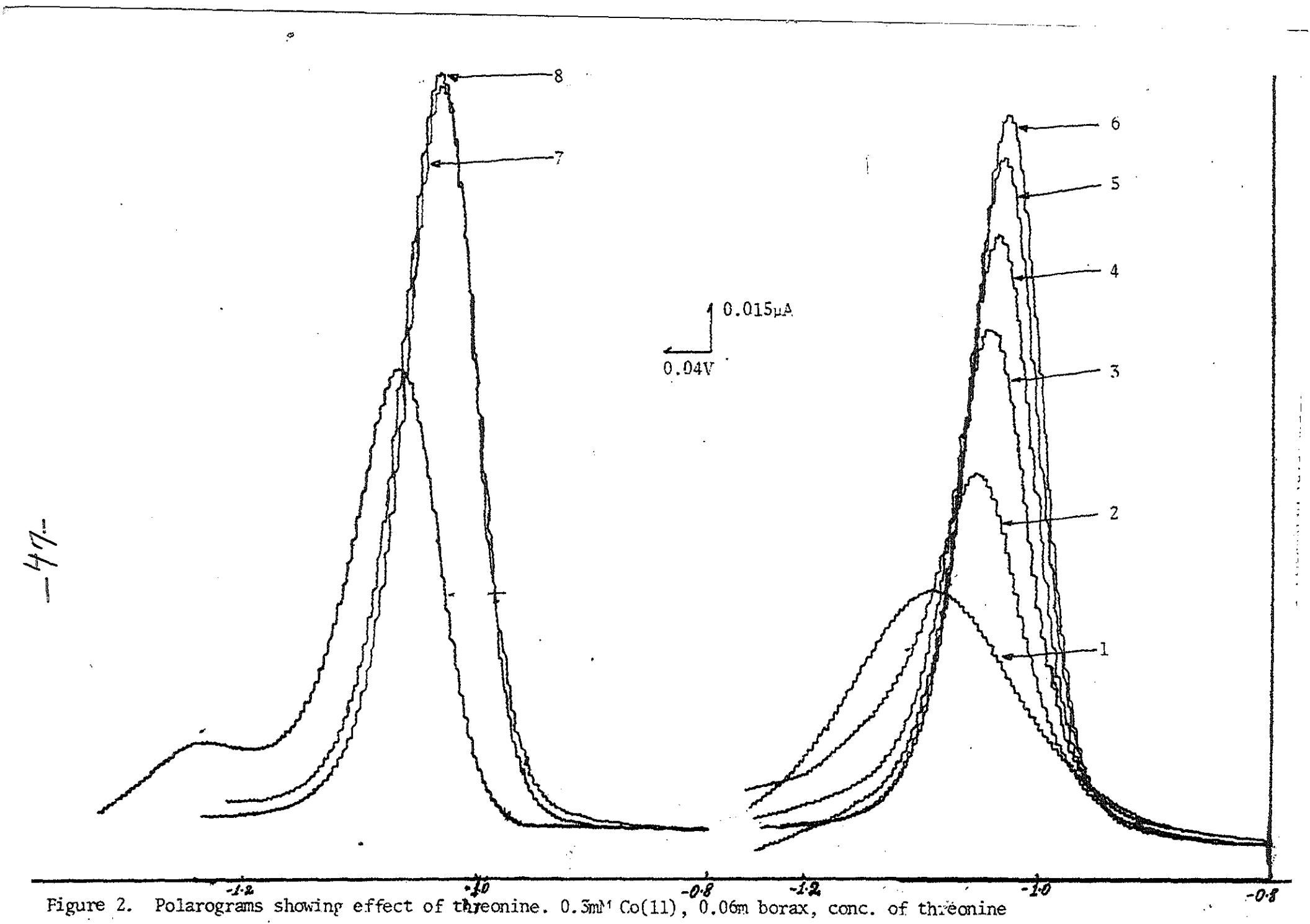

Figure 2. Polarograms showing effect of threonine. 0.3mM Co(11), 0.06m borax, conc. of threonine

[illegible] 0.5, 5, 0.5, 6, 0.75, 7, 0.994, 8, 2.25, 9, 15 mM. Commencing potential -1.0V

in threonine. With a further increase of threonine (threonine concentration greater than 1.5×10^{-3}M) the peak potential shifts back to more negative values, although still more positive than the aquo cobalt reduction peak potential. The peak current also decreases (see Table (3)), and a second wave appears as shown in figure (2) when the threonine concentration is 0.015M.

Table 1

[thr] M	$i_p u$ Amps	$-E_p$
-	0.175	1.29
2.5×10^{-5}	0.215	1.248
7×10^{-5}	0.305	1.244
10^{-4}	0.37	1.236
2×10^{-4}	0.435	1.232
2.5×10^{-4}	0.49	1.232
3.5×10^{-4}	0.586	1.232
4×10^{-4}	0.62	1.232
5×10^{-4}	0.665	1.232
7×10^{-4}	0.73	1.232
10^{-3}	0.77	1.232

Table 2

[thr] M	$i_p u$ Amps	$-E_p$ V
-	0.79	1.292
5×10^{-5}	1.17	1.252
10^{-4}	1.418	1.244
1.5×10^{-4}	1.628	1.24
3×10^{-4}	1.928	1.236
5×10^{-4}	2.2	1.232
7.5×10^{-4}	2.322	1.229
9.375×10^{-4}	2.355	1.228
1.225×10^{-3}	2.397	1.228

Table 3

$[thr]_M$	$i_p u$ Amps	$-E_p$ V
-	1.26	1.293
$> 5 \times 10^{-5}$	1.55	1.256
10^{-4}	1.988	1.246
2×10^{-4}	2.413	1.232
4×10^{-4}	2.988	1.232
5×10^{-4}	3.05	1.232
6.5×10^{-4}	3.115	1.232
8×10^{-4}	3.2	1.232
10^{-3}	3.275	1.232
2×10^{-3}	3.2125	1.236
4×10^{-3}	3.0125	1.24
5×10^{-3}	2.8875	1.246

Tables showing the variation of peak current and potential as a function of threonine concentration in 0.06M borax at constant cobalt concentrations. Concentration of Co(II); 10^{-4}M table (1), 3×10^{-4}M table (2), and 4×10^{-4}M table (3)

4.3.2. Effect of pH

Since boric acid has no effect on the reduction peak of Co(II) in 0.06M sodium tetraborate (54) a study of the pH dependence of the Co(II) - threonine

reduction was made by adding boric acid to the system containing 0.06M $Na_2B_4O_7$, 4 x 10^{-4}M $CoSO_4$, and using three constant concentrations of threonine, viz, 10^{-3}M, 2 x 10^{-3}M and 4 x 10^{-3} threonine. In line with threonine concentration dependence of the peak current, with rising pH, the peak current also increases (see Fig. (3)). The peak potential is shifted toward more positive values with increasing pH (see table (4)).

Table 4

$[H_3BO_3]$ M	pH	$i_p\mu$ Amps	$-E_p$ V
-	9.2	3.3	1.226
0.1	8.7	3.1	1.224
0.2	8.4	2.885	1.228
0.26	8.15	2.52	1.221
0.36	7.9	2.153	1.224
0.48	7.5	1.677	1.226
0.6	7.1	1.46	1.232
0.88	6.5	1.38	1.252
Saturated	6	1.358	1.256

Table 5

$[H_3BO_3]$ M	pH	$i_p u$ Amps
-	9.2	3.15
0.05	8.9	3.117
0.1	8.7	3.27
0.2	8.4	3.173
0.3	7.75	2.988
0.49	7.45	2.595
0.54	7.3	2.4
0.6	7.2	2.205
0.88	6.55	1.515
Saturated	6	1.38

Table 6

$[H_3BO_3]$ M	pH	$i_p u$ Amps
-	9.2	3.365
0.08	8.85	3.308
0.2	8.4	3.26
0.4	7.75	2.6
0.5	7.4	2.165
0.6	7.2	1.673
0.8	6.8	1.425
Saturated	6	1.283

Tables (4), (5), & (6): Variation of peak current with pH for the systems: 4×10^{-4}M Co(II), 0.06M borax: and 10^{-5}M threonine table (4), 2×10^{-3}M threonine, table (6) and 4×10^{-3}M threonine table (5).

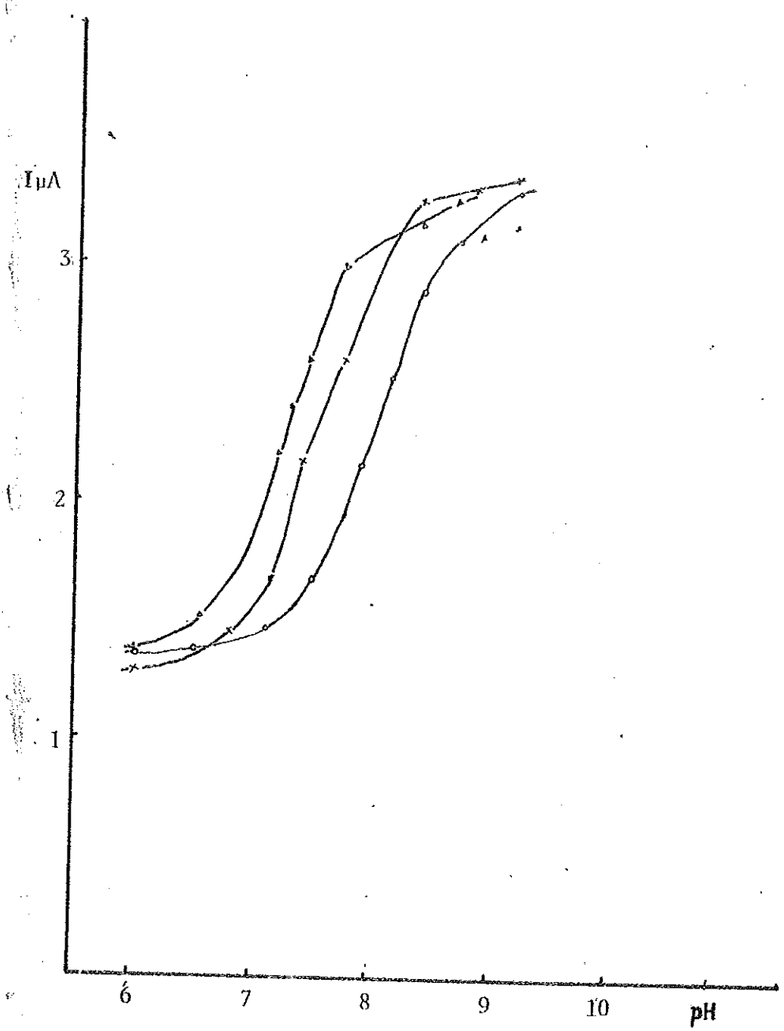

Figure 3. Plot of peak current Vs pH in 0.4mM Co(11), 0.06m borax: threonine conc., 1(o), 3(x), 4(V)mM.

4.3.3. Effect of Co(II) Concentration

The effect of Co(II) concentration on the Co(II) - threonine reduction was studied in 0.4M boric acid, 0.06M borax (pH 7.8) medium by varying the Co(II) concentration up to 10^{-3}M.4 x 10^{-3}M and 4 x 10^{-4}M constant concentrations of threonine were maintained. The plots of peak current against cobalt concentration are given in Figure (4). As shown in this figure the peak current increases linearly with metal concentration for a given threonine concentration. The same concentration of metal differing concentrations of threonine yield different peak currents. The higher the threonine concentration the higher the peak current. This effect of threonine concentration however does not extend to higher concentrations. Table (7) includes peak currents observed in 0.01M threonine, 0.2M boric acid, 0.06M borax (pH 8.4) medium. These values are very close to those obtained in the 4 x 10^{-3}M threonine system.

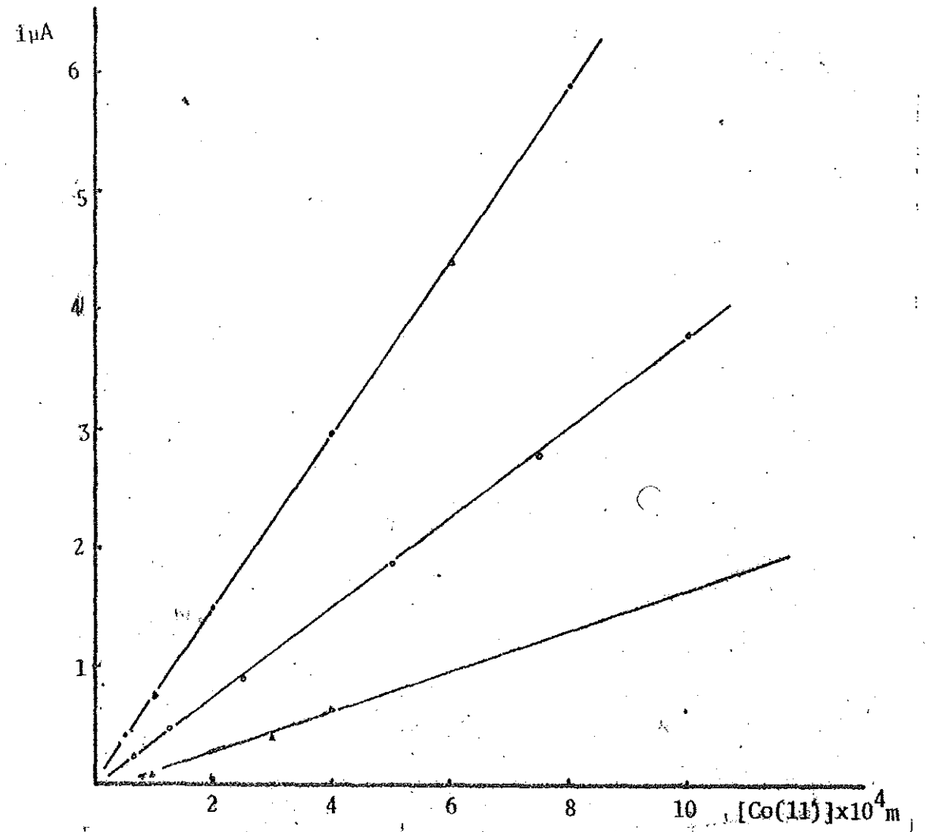

Figure 4. Variation of peak current as a function of Co(11) conc in 0.4m boric acid and 0.06m borax. Threonine conc., 0(▽), 0.4mM(0), 4mM(.)

Table 7

$[Co^{2+}]M$	i_p u Amps
5×10^{-5}	0.4
10^{-4}	0.776
2×10^{-4}	1.288
4×10^{-4}	3.08
6×10^{-4}	4.44
8×10^{-4}	5.956
10^{-3}	7.552

Variation of peak current with cobalt concentration in 0.01M threonine, 0.2M H_3BO_3, 0.06M $Na_2B_4O_7$.

4.3.4 Characteristics of the Co(II) - Threonine Reduction

The dependence of the DC polarographic limiting current on drop time was carried out in order to elucidate the reduction mechanism of the Co(II) - threonine complex. Because the nature of the reduction can depend on the concentration of threonine, the current drop time dependence studies were made at a concentration of threonine corresponding to the linearly increasing portion, as well as the plateau region of current versus threonine concentration plot in Figure (1); i.e threonine

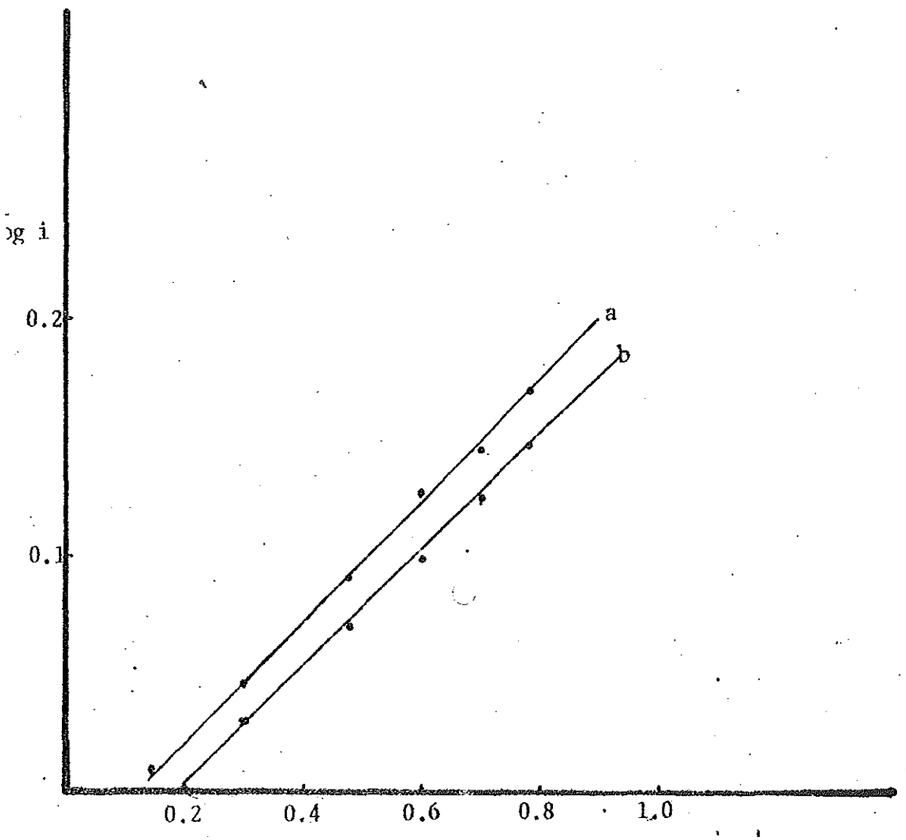

Figure 5: Plot of log Vs log h: 0.4mM Co(11), 0.06m borax
a) 0.5mM, b) 1mM threonine.

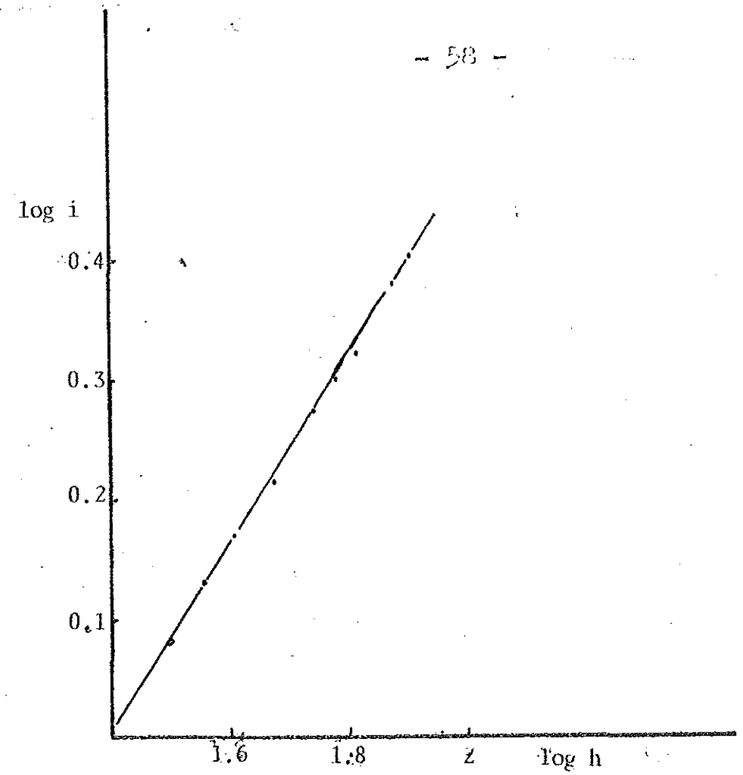

Figure 6: Plot of log i Vs log h:
0.4mM Co(11), 0.15mM threonine, 0.06m borax

concentrations of 1.5×10^{-4}M and 10^{-3} respectively, both in 4×10^{-4} $CoSO_4$, 0.06M $Na_2B_4O_7$ medium. The slopes of the log i versus log t plots are 0.26 and 0.24 (see Figure (5)) for the system 1.5×10^{-4}M and 10^{-3}M in threonine respectively (measurements done at 25°C). The current drop time dependence of the 1.5×10^{-4}M threonine system at 0°C gave a slope of 0.22.

The variation of the DC polarographic limiting current on mercury reservoir hight was also investigated for the system 1.5×10^{-4}M threonine, 4×10^{-4}M $CoSO_4$, 0.06M $Na_2B_4O_7$. The slope of the log i versus log h plot (see Figure (6) was found to be 0.79.

4.4. Discussion

A study of the character of the Co(II) - threonine polarographic reduction at a ligand concentration of 1.5×10^{-4}M threonine and 10^{-3}M threonine (see Figure(1)) gave a slope of 0.26 and 0.24 respectively, for the log i - log t plot. This implies that the reduction is both diffusion and kinetic controlled (55). Provided there is kinetic competition at 25°C, the reduction ought to be purely kinetic at lower temperature. However the slope of the log i - log t plot at 0°C for the 1.5×10^{-4}M threonine system is 0.22. If kinetic currents are observed in the reduction of metal complexes, then there

must exist an equilibrium mixture of several complexes of the same metal ion with different number of ligands (55). Therefore the current magnitude of kinetic waves is always unexpectedly small as are adsorption waves (56, 57). This is unlike the Co(II) - threonine reduction.

Threonine concentration has a great effect on both the peak current and potential as shown in tables (1), (2) and (3). A concentration ratio as small as 1:8 (ligand to metal) shifts the peak potential to more positive value by 35 millivolts. (As compared to the peak potential of the simple metal ion) and it also increases the peak current by about 23%. At higher ligand to metal ratio (from 1:1 to 80:1, see Figure 4) there still is only one peak which again appears anodic to the simple metal ion reduction potential. If one assumes that, at low ligand to metal ratio, only part of the metal ion is complexed, whereas the rest remains uncomplexed, then one would have expected at least two waves, one corresponding to the reduction of the complex and another to the reduction of the simple metal ion. Since this is not observed, and since there is no distinct difference in the polarographic behaviour at very low and moderate ligand to metal ratios, it is difficult to conclude from this study alone, whether or not the shift in the peak potential due to changes in

the ligand concentration is due to complexation.

In view of the fact that the peak current is always higher in the presence of threonine than without, (see Figure (4)), it may be concluded that the reduction is not diffusion controlled.

An increase in pH shiftsthe reduction peak potential to more positive values (see table (4)) and also leads to an increase in peak current (see Figure (3)). The effect of pH is to be seen in light of its effect on the relative distribution of threonine between its zwitterion and anion forms. The zwitterion is normally not a good complexing species. A number of studies have indicated that it is, in general, the anion form of amino acids that complexes (58, 59, 60, 61). The pH effect observed in this work also shows that the species responsible for the increased peak current and positive shift of peak potential must be the anion form of threonine (threoninate).

4.5. Conclusions

The behaviour of the Co(II) - threonine system has been found to be anomalous in that there is observed a positive shift in peak potential and an increase in the peak current on addition of threonine while at the same time exhibiting only one peak at low and moderate ligand concentrations. A second wave appears only when the threonine concentration is as high as 0.015M. The indications so far are that the Co(II) - threonine reduction is mainly catalytic in nature, although a more conclusive statement must await answers to questions relating to the reason for the large shifts in peak potential for small additions of ligand, the appearance of only one wave at low and moderate ligand concentrations with similar polarographic behaviours, but of two waves at very high ligand concentration.

It is felt that coupling of the above investigation with spectroscopic studies could shed some light regarding the complexation of Co(II) with threonine and that further work at high concentrations may be very useful in understanding and characterizing the reduction process.

One conclusion that can be made, however, is that there is a clear possibility of using differential pulse polarographic technique for the analytical determination of threonine.

4.6. Results of Ni(II) - Threonine System

The dependence of the double - wave of Ni(II) - threonine polarographic reduction has been studied as a function of threonine concentration, Ni(II) concentration, pH and ionic strength. The dependence of the limiting current on the mercury reservoir height, as well as on drop time have also been studied.

4.6.1. Effect of Threonine Concentration

The effect of threonine concentration on the polarograms of the Ni(II) - threonine system in borate medium was investigated in 0.01M and 0.06M sodium tetraborate. The polarograms are given in figures (1) and (2), and the peak current dependences are given in Figure (3) and (4) respectively.

The peak potential for 2 x 10^{-4}M Ni(II) in 0.01M borax is -0.988V and its peak current is 1.00 μ amps. When the solution is also 8 x 10^{-5}M with respect to threonine the polarogram gives only one peak at a potential which is 40 millivolts shifted in the positive direction. A prewave begins to appear (at -0.932V) when the threonine concentration is 10^{-4}M. The peak potentials of the prewave, as well as of the second wave are different from that of the simple metal ion, for all threonine concentrations as shown in Table 1.

Figure 1. Ni(II) waves in 0.01M broax, 0.2mM Ni(II), [thr] = 1, 0; 2,8 x 10^{-3}; 3, 0.08; 4, 0.1; 5, 0.2; 6, 0.4; 7, 0.5; 8, 0.8; 9, 1; 10, 2; 11, 4; 12, 8; mM.

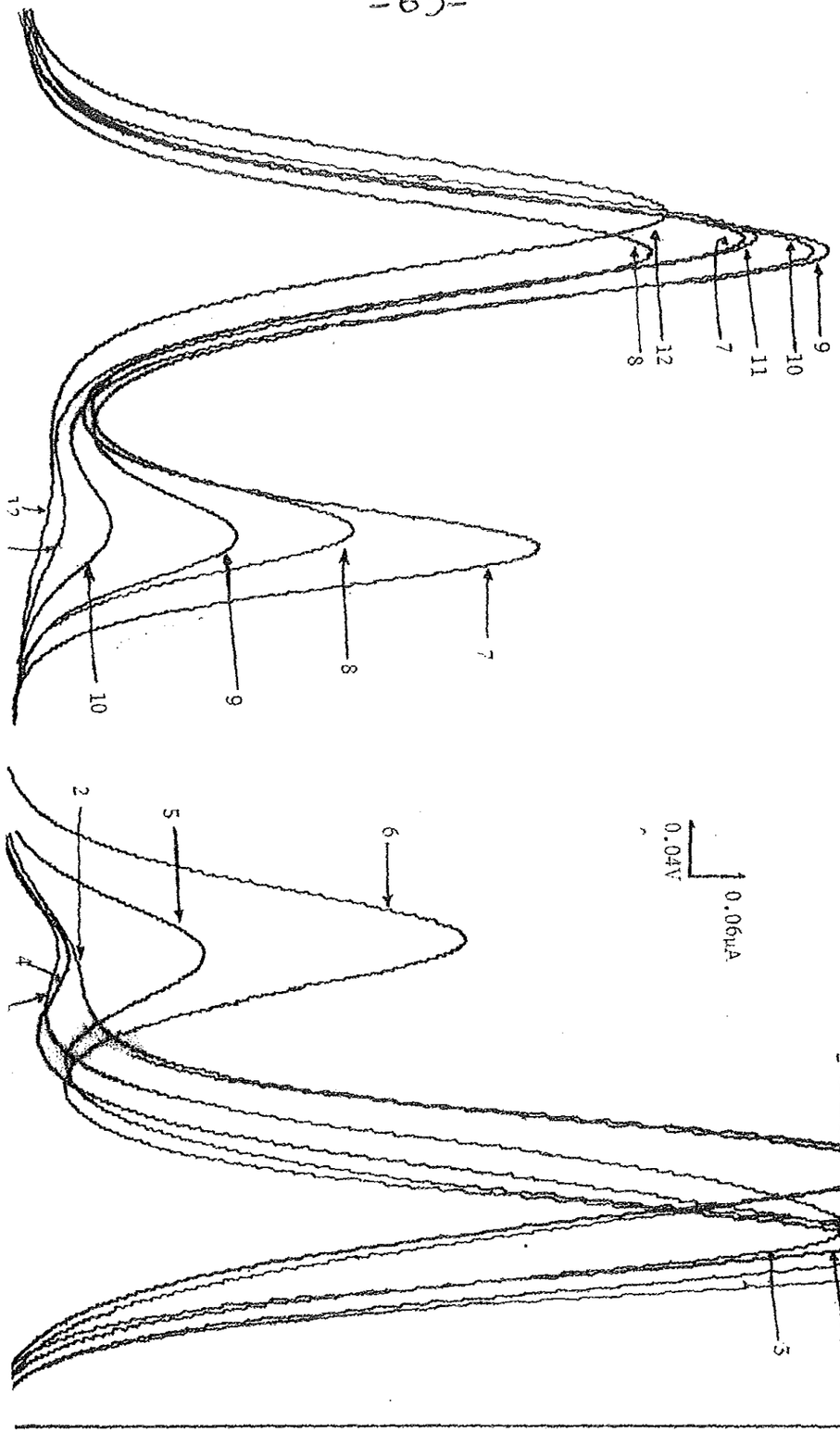
12
11
10
9
8
7
6
5
4
3
2
1
0.04V
0.06μA

Figure 2. Ni(II) waves in 0.6M borax, 0.2mM Ni(II),
0 [thr] = 1, 1; 2, 2; 3, 3; 4, 4; 5, 5;
6, 6; 7, 7; 8, 8; 9, 9; 10, 10; mM.

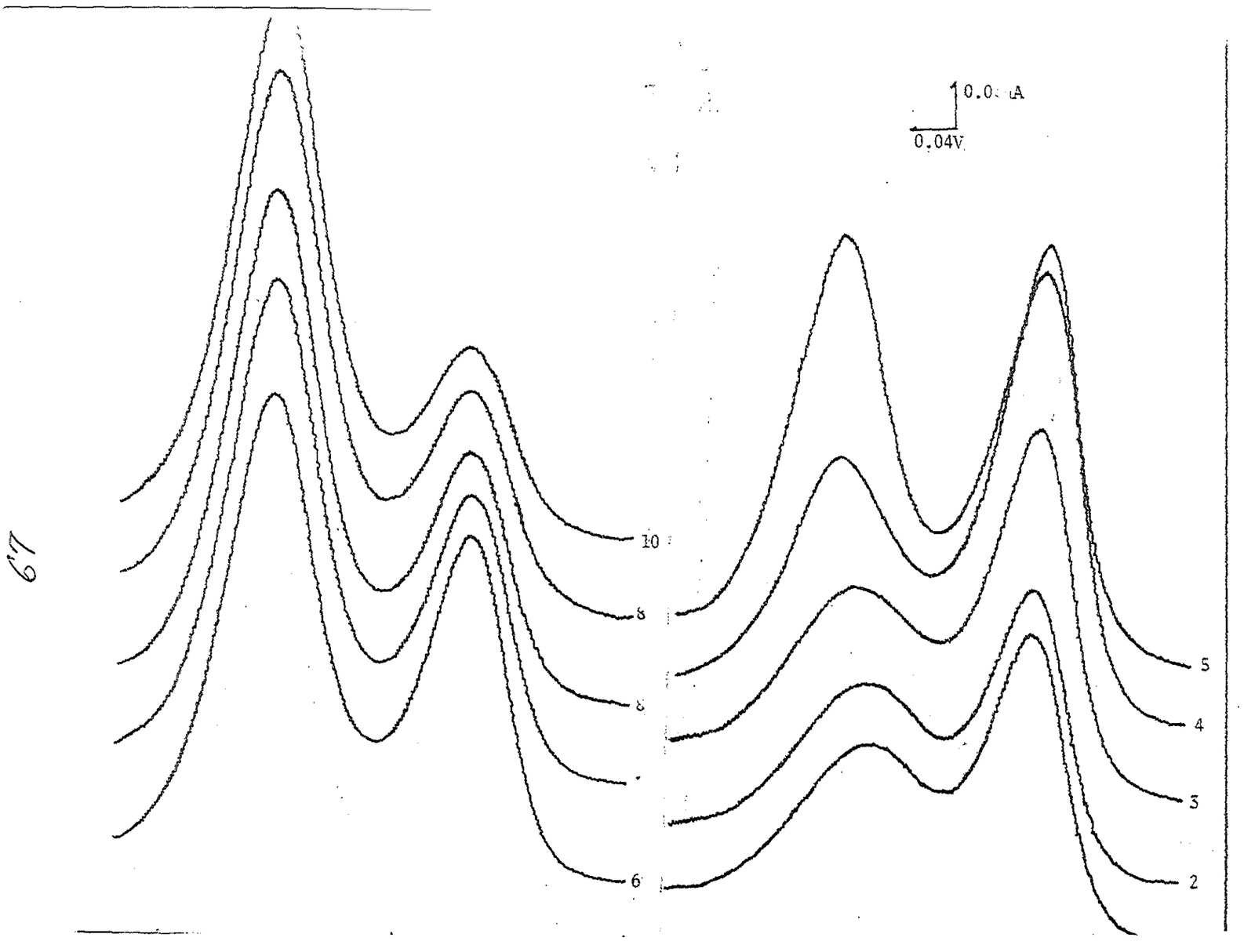
0.0 μA
0.04V
10
8
8
6
5
4
3
2

Table 1. Peak Current and Potential Dependences of Ni(II)-Threonine Waves on Threonine Concentration in 0.01M Borax

[Thr] M	i_{p_1} u Amps	$-E_{p_1}$ V	i_{p_2} u Amps	$-E_{p_2}$ V
-	1.002	0.988	-	-
$8x10^{-5}$	0.927	0.946	-	-
10^{-4}	0.977	0.932	0.078	1.04
$2x10^{-4}$	1.151	0.924	0.228	1.042
$4x10^{-4}$	0.947	0.936	0.516	1.054
$5x10^{-4}$	0.567	0.928	0.687	1.044
$8x10^{-4}$	0.366	0.942	0.792	1.054
10^{-3}	0.243	0.936	0.882	1.044
$2x10^{-3}$	0.099	0.944	0.858	1.048
$4x10^{-3}$	-	-	0.804	1.052
$8x10^{-3}$	-	-	0.708	1.072

The polarograms of the Ni(II) - threonine system in 0.06M sodium tetraborate, shown in Figure 2, give lower peak currents than those in 0.01M sodium tetraborate. In 0.06M sodium tetraborate, the simple metal ion peak potential is -1.06V while that for the prewave and second waves are about -0.94V and -1.11V respectively (Table 2). The peak current dependences on threonine concentration are shown in Figure 4.

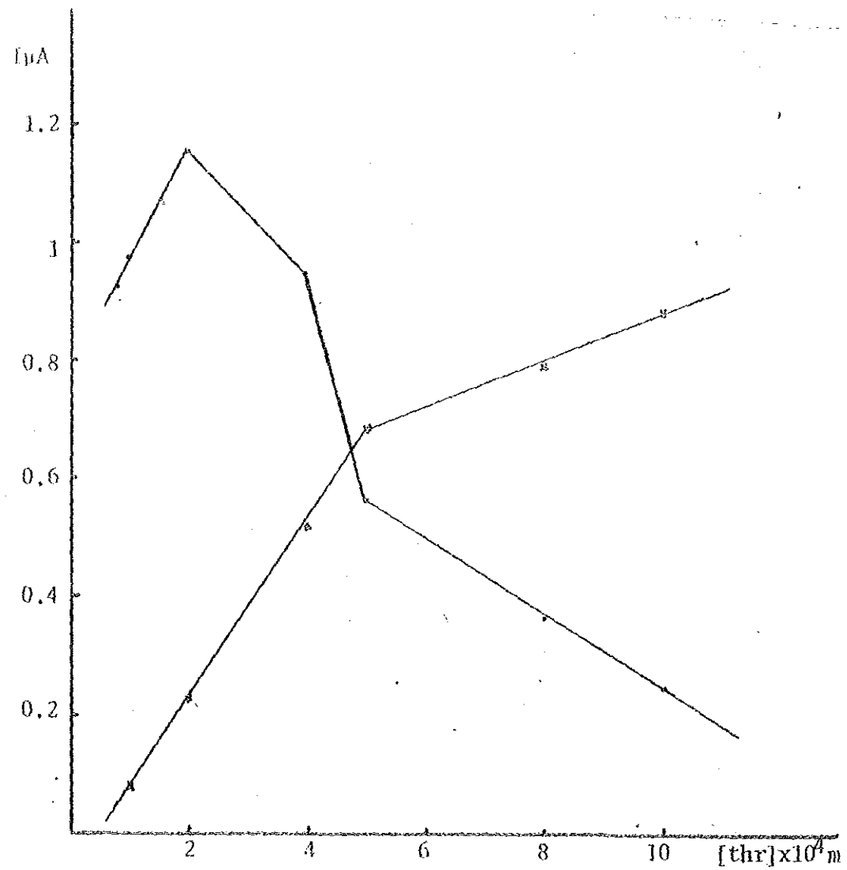

Figure 3. Plot showing peak current dependence on threonine conic. in 0.01m borax, 0.2mM Ni(11). Prewave peak current (·), second wave peak current(x).

Prewaves have so far been applied for an indirect quantitative determination of polarographically non-active substances (62, 63, 33).

Table 2. Variation of the Peak Currents and Peak Potentials as a Function of Threonine Concentration, in 0.06M Borax, when Ni(II) is $2x10^{-4}$M

[Thr] M	i_{p_1} μ Amps	$-E_{p_1}$ V	i_{p_2} μ Amps	$-E_{p_2}$ V
-	0.255	1.06	-	-
10^{-4}	0.384	0.936	0.234	1.068
$2x10^{-4}$	0.366	0.936	0.234	1.074
$3x10^{-4}$	0.465	0.936	0.252	1.088
$4x10^{-4}$	0.606	0.936	0.321	1.107
$5x10^{-4}$	0.51	0.938	0.498	1.11
$6x10^{-4}$	0.438	0.939	0.615	1.11
$7x10^{-4}$	0.363	0.939	0.636	1.11
$8x10^{-4}$	0.312	0.940	0.648	1.11
$9x10^{-4}$	0.282	0.942	0.684	1.11
$10x10^{-4}$	0.24	0.944	0.687	1.11

A similar attempt to determine the optimum conditions in which the Ni(II) - threonine prewave can be used for the quantitative determination of threonine was made (see Figure 6). From Figure 5 and 6 it is evident that the prewave peak current increases and then levels off to a plateau in the concentration range considered, i.e. from 10^{-5}M to $2x10^{-4}$M threonine. At low concentrations from 10^{-5} to 10^{-4}M threonine the prewave peak current is

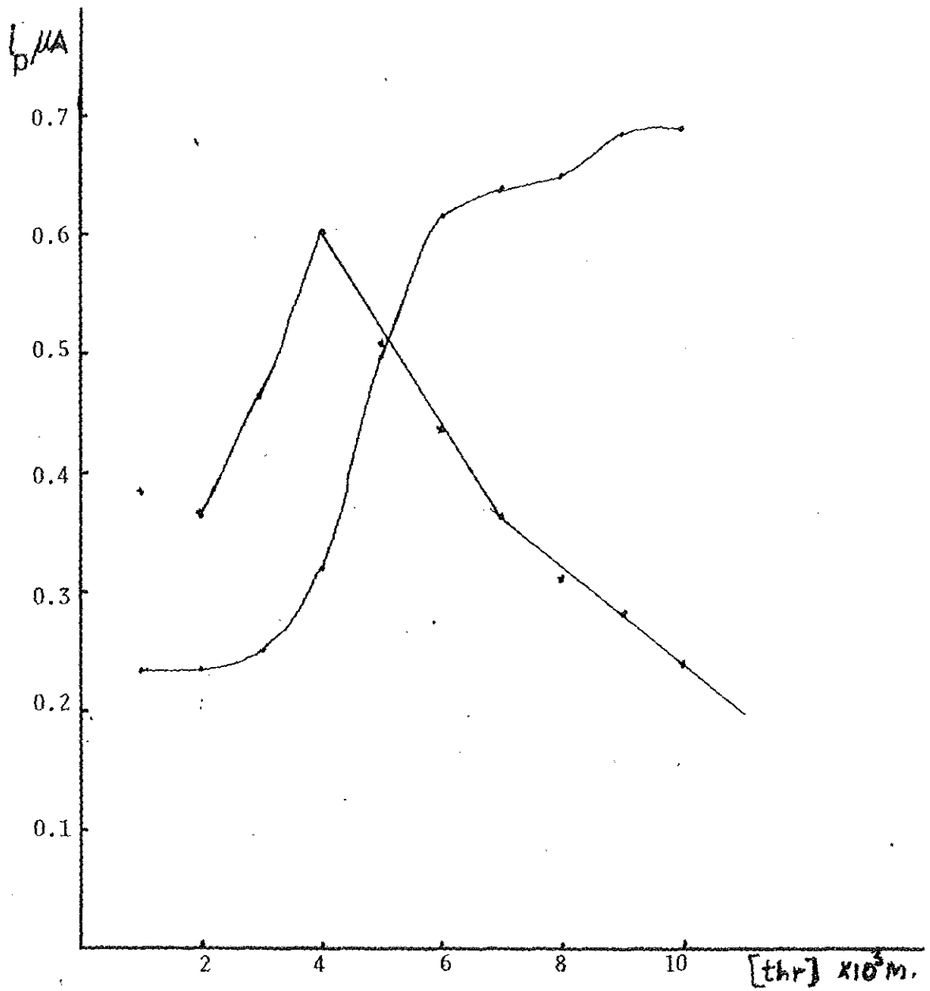

Figure 4. Plot of table (2), showing peak current dependence on threonine conc. prewave peak current (x), second wave peak current (·).

a linear function of the threonine concentration. At still lower concentrations less than 10^{-5}M threonine, the prewaves are not resolved enough to be suitable for analysis.

Table 3. Values of Peak Currents and Potentials as a Function of Threonine Concentration Ni(II), 2×10^{-4}M, 0.06M Borax.

[Thr] M	i_{p_1} µAmps	$-E_{p_1}$ V	i_{p_2} µAmps	$-E_{p_2}$ V
1.2×10^{-5}	0.085	0.947	0.263	1.068
1.6×10^{-5}	0.098	0.947	0.258	
2.4×10^{-5}	0.13	0.947	0.243	
2.8×10^{-5}	0.143	0.947	0.248	
3.2×10^{-5}	0.159	0.947	0.248	1.07
4×10^{-5}	0.196	0.942	0.255	
4.8×10^{-5}	0.224	0.942	0.255	
5.6×10^{-5}	0.253	0.942	0.255	
6.4×10^{-5}	0.274	0.942	0.25	
7.2×10^{-5}	0.298	0.942	0.254	1.07
8×10^{-5}	0.319	0.942	0.251	
8.8×10^{-5}	0.346	0.941	0.25	1.072
9.6×10^{-5}	0.37	0.941	0.253	
10^{-4}	0.39	0.941	0.25	
1.125×10^{-4}	0.41	0.930	0.233	
1.25×10^{-4}	0.443	0.931	0.25	
1.5×10^{-4}	0.504	0.931	0.275	
1.75×10^{-4}	0.545	0.932	0.294	1.073
2×10^{-4}	0.57	0.932	0.293	

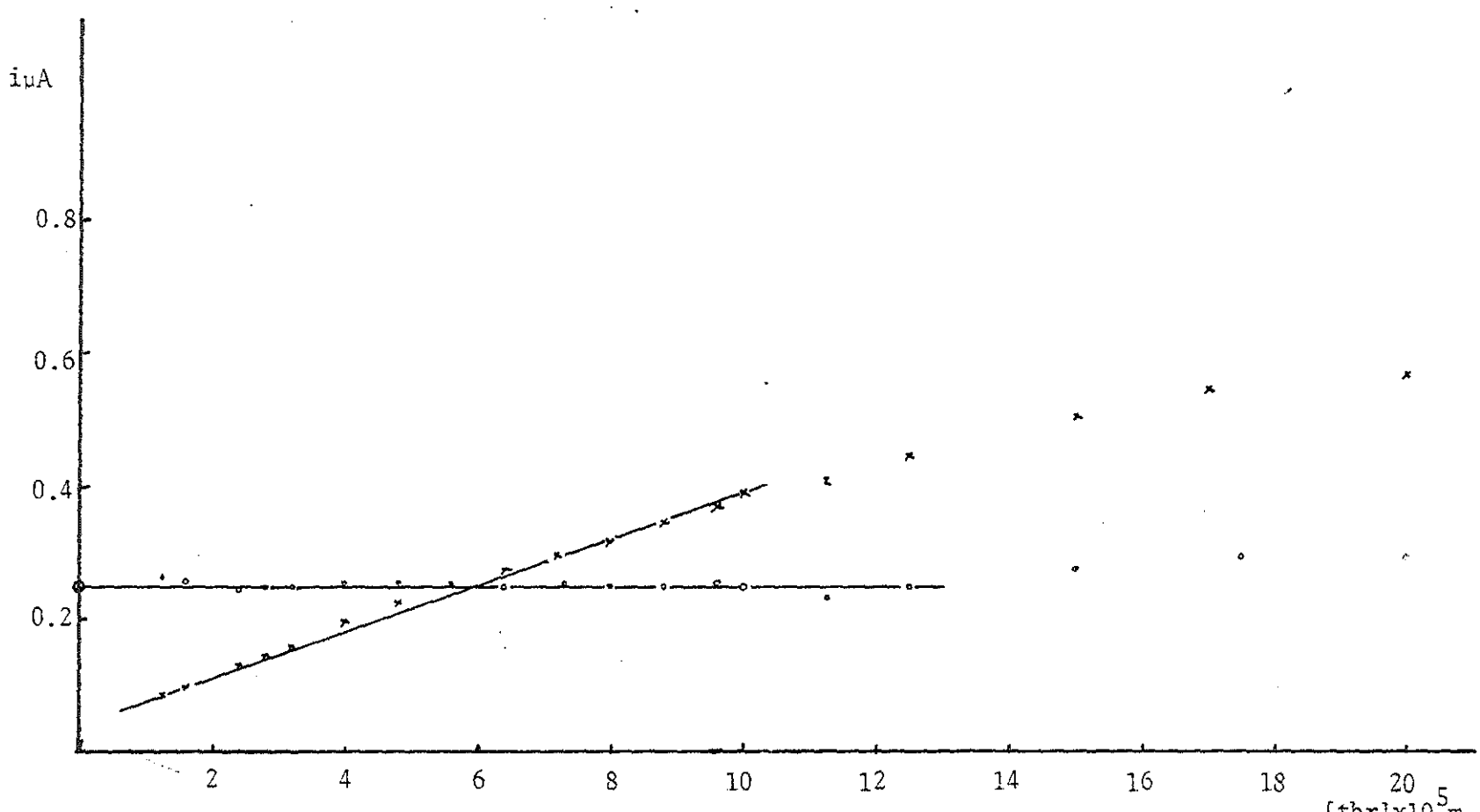

Figure 5. Plot os prewave (x) and second wave (o) dependences on threonine conc. in 0.06m borax and 0.2mM Ni(11).

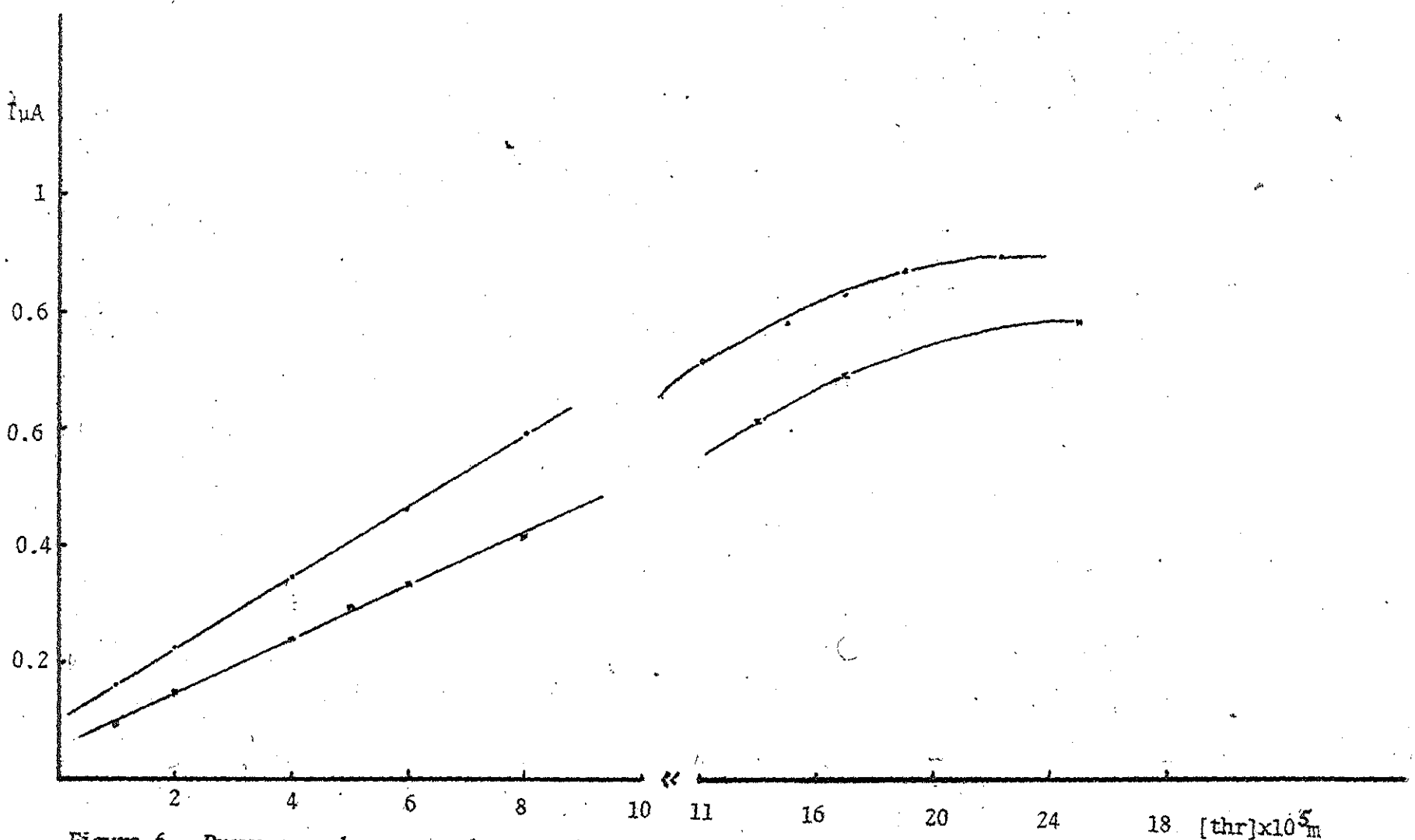

Figure 6. Prewave peak current dependence on threonine conc. in 0.2mM Ni(11), 0.03m borax, 0.09m KNO_3(.) and 0.2mM Ni(11), 0.06m borax (.)

4.6.2. Effect of Ni(II) Concentration

The prewave peak current, Table 4, shown in Figure 7, as a function of Ni(II) concentration was investigated in 0.09M KNO_3, 0.03M $Na_2B_4O_7$, because higher peak currents, and fairly well resolved waves were obtained in this supporting electrolyte. The threonine concentration was kept successively constant at $4x10^{-5}$M, $8x10^{-5}$M and $1.2x10^{-4}$M. As shown in Figure 7, the prewave peak current levels off to a plateau in all cases. A representative set of polarograms is shown in Figure 8.

Table 4. Prewave Peak Current Dependence on Ni(II) concentration in 0.09M KNO_3, 0.03M borax supporting Electrolyte, when the Threonine Concentrations are $4x10^{-5}$M, $8x10^{-5}$M and $1.2x10^{-4}$M Threonine.

$[Ni^{2+}]$ M	$4x10^{-5}$M Thr	$8x10^{-5}$M Thr	$1.2x10^{-4}$M Thr
$2.5x10^{-5}$	0.19	0.138	0.12
$5x10^{-5}$	0.276	0.27	0.228
10^{-4}	0.348	0.422	0.44
$2x10^{-4}$	0.368	0.574	0.684
$3x10^{-4}$	0.376	0.636	0.763
$4x10^{-4}$	0.388	0.664	0.803
$5x10^{-4}$	0.13	0.686	-
$6x10^{-4}$	-	-	0.84

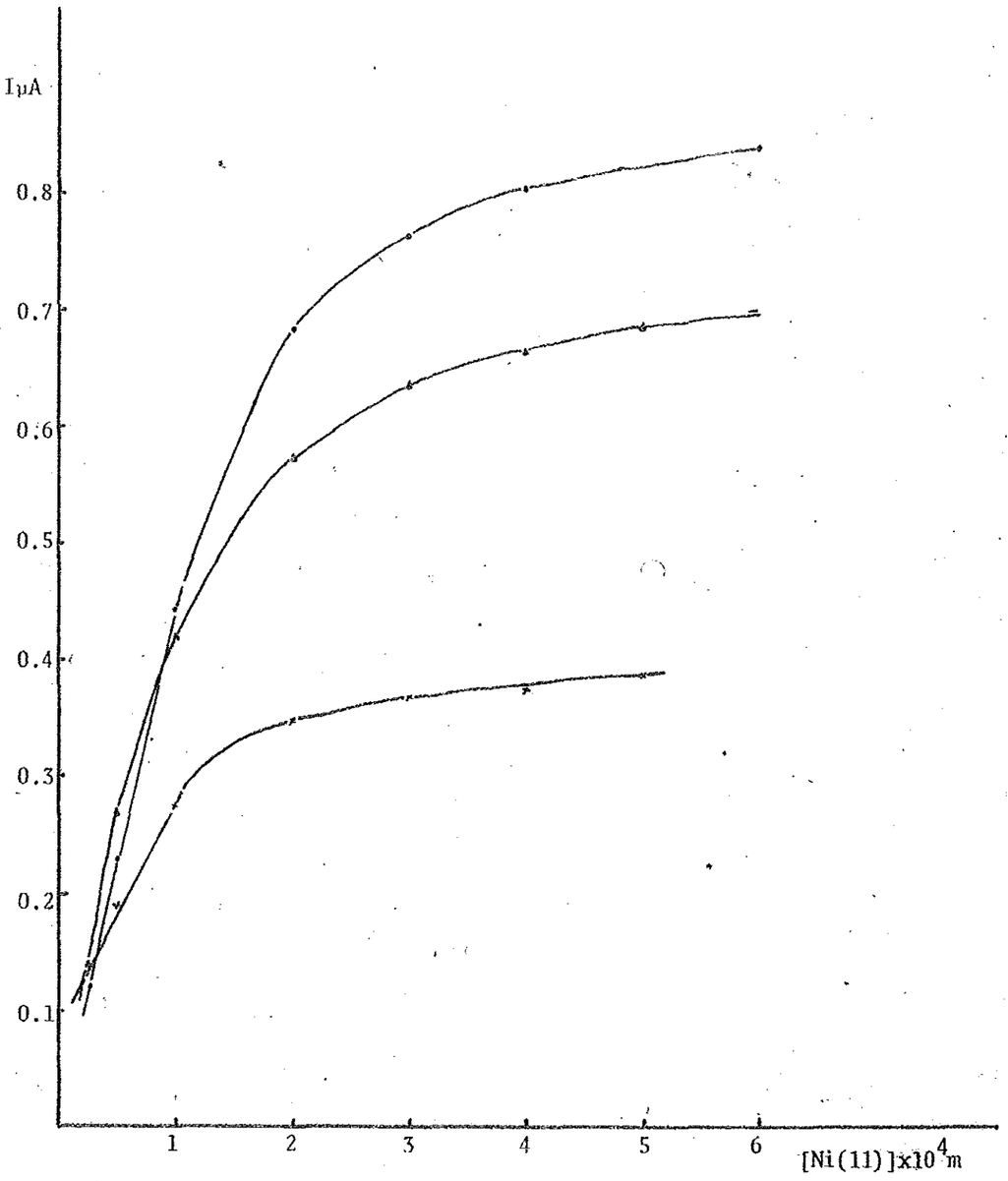

Figure 7. Variation of prewave peak current with conc. of Ni(11) in 0.09m KNO_3, 0.03m borax. threonine conc., 0.04(x), 0.08(Δ), 0.12(·)mM.

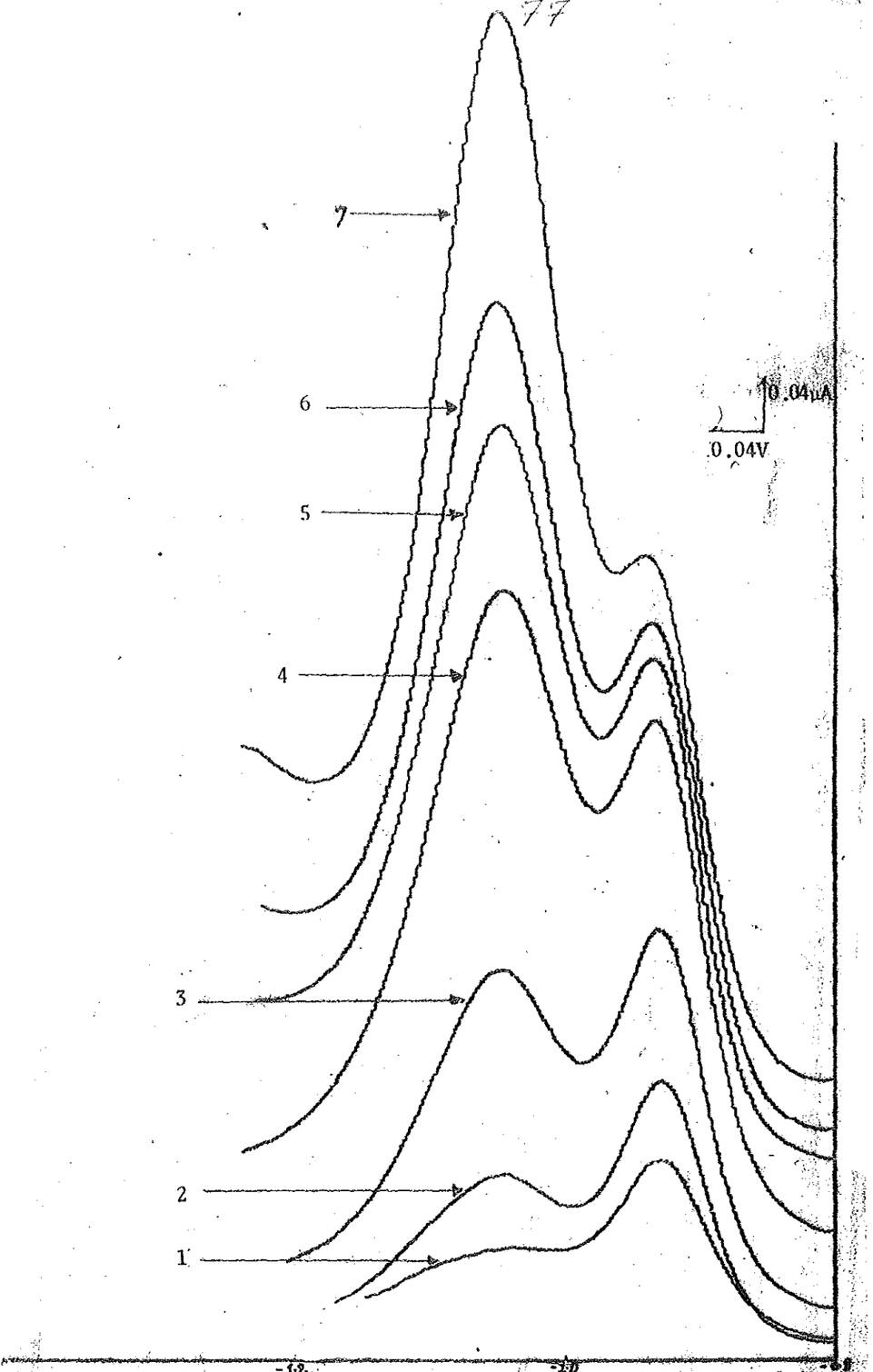

Figure 8. Polarograms of Ni(11) in 0.03m borax, 0.09m KNO_3, 0.04mM threonine Ni(11) conc., 1, 0.025; 2,0.05; 3,0.1; 4,0.2; 5,0.3; 6, 0.4; 7,0.5mM

4.6.3. Effect of Ionic Strength

The effect of ionic strength on the Ni(II) reduction was studied in 0.06m sodium tetraborate, but varying concentration of potassium nitrate. As shown in Figure 9, the peak current decreases, with increasing ionic strenth, while there is no significant shift in the peak potential.

The dependence of the Ni(II) - threonine reduction on the ionic strength was then studied by varying the sodium tetraborate concentration, as this has only little influence on the pH of the solution. The threonine and metal concentrations were kept constant at $4x10^{-5}$M and $2x10^{-4}$M respectively.

Table 5. Dependence of Peak Currents and Potentials of Ni(II) - threonine on Concentration of sodium Tetraborate. $[Ni^{2+}] = 2x10^{-4}$M, [Thr] = $4x10^{-5}$M

$[Na_2B_4O_7]$	i_{p_1}	$-E_{p_1}$	i_{p_2}	$-E_{p_2}$
0.06	0.248	0.948	0.302	1.074
0.05	0.314	0.948	0.43	1.054
0.04	0.404	0.95	0.52	1.024
0.03	0.475	0.956	0.616	1.016
0.02	-	-	-	-
0.01	-	-	-	-

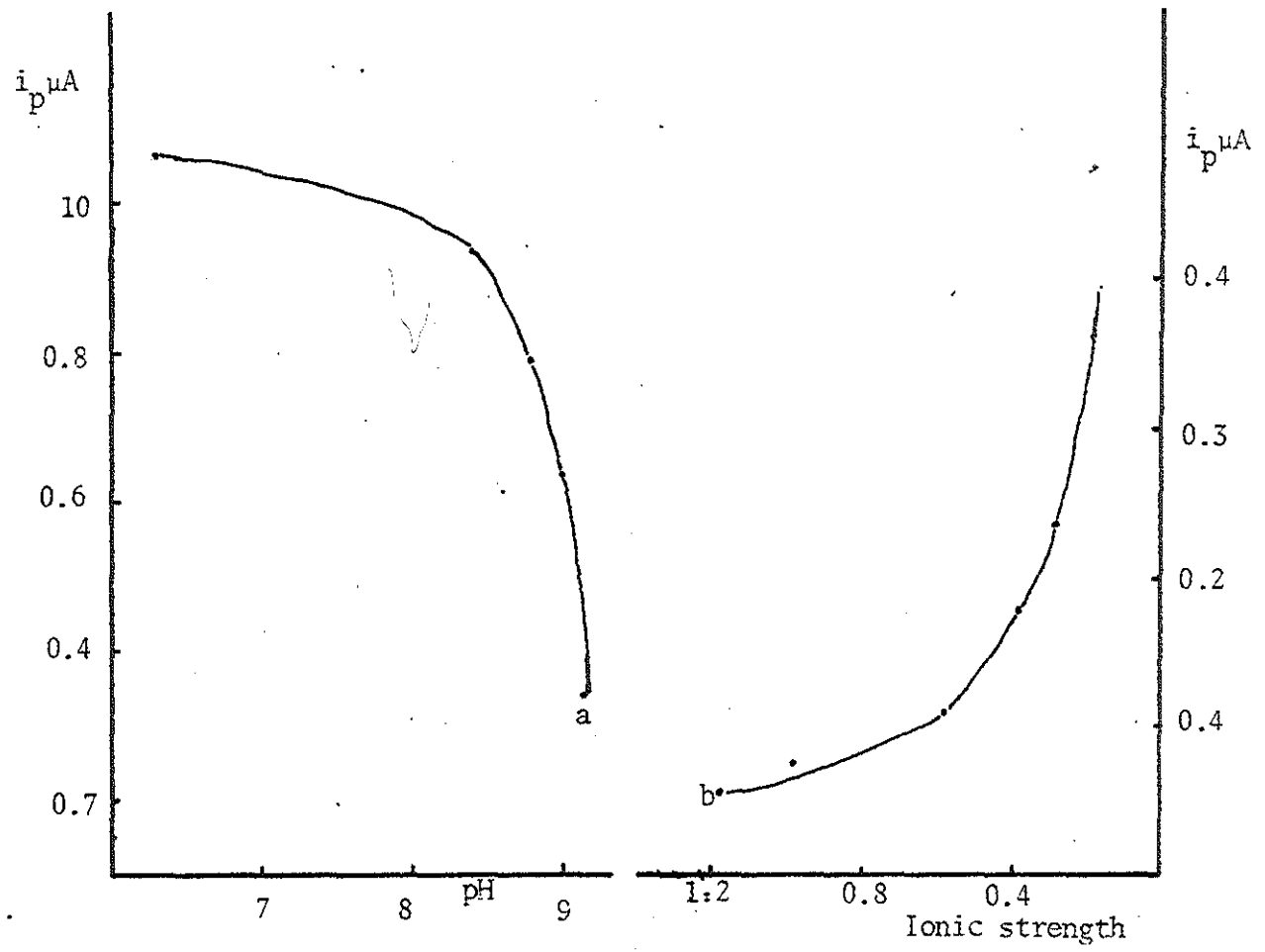

Figure 9. Peak current dependence of 0.2mM Ni(11) on a) pH, b) ionic strength.

Figure 10. Polarograms of 0.2mM Ni(II), 0.04mM threonine in varying conc. of borax. 1, 0.06; 2, 0.05; 3, 0.04; 4, 0.03; 5, 0.02; 6, 0.01; 7, 0.01M borax, 0.15M KNO_3; 8, 0.03M borax, 0.09M KNO_3

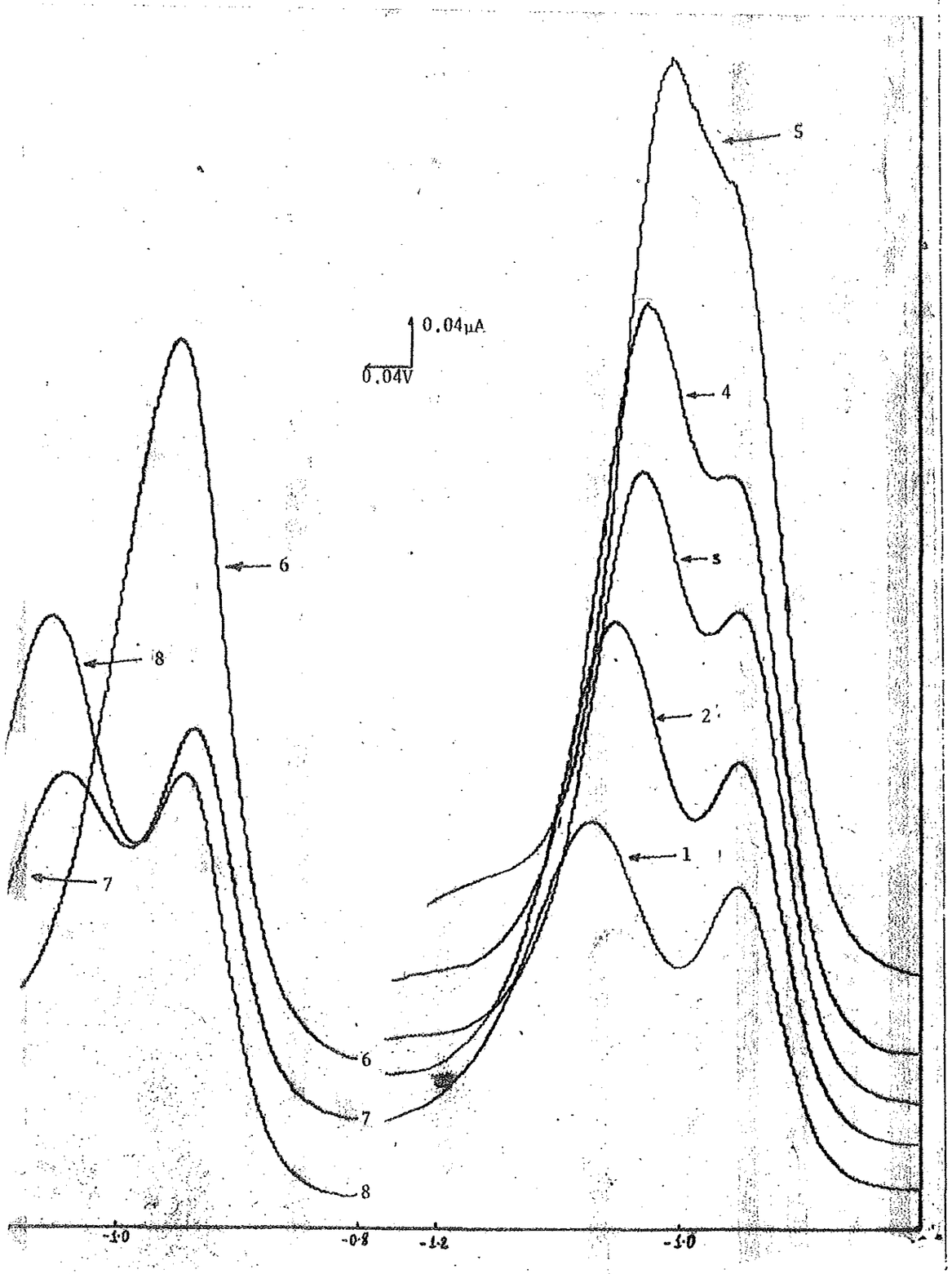
0.04μA
0.04V
5
4
3
2
1
6
8
7
6
7
8
-1.0
-0.8
-1.2
-1.0

Although it can be seen that there are two peaks when the concentration of sodium tetraborate is 0.02M (see Figure 10), they are not resolved enough to enable current and potential measurements. At 0.01M sodium tetraborate, the two waves coalesce to form just one peak, whose peak potential is -0.948V and peak current is 0.592 μ amps. When this very solution is made 0.15M in potassium nitrate (Figure 10), it gives a prewave at -0.936V of 0.318 μ amps. The sum of these two peak currents is 0.598 μ amps, which is about equal to the parent non-separated peak. Both the separation and peak currents are dependent on the ionic strength. At the same ionic strength a higher peak current is recorded in a mixture of KNO_3 and borax, than in borax alone (see Figure 11). The loss in the resolution of the peaks seems largerly to be the result of the shift of the second wave towards more positive potential when the sodium tetraborate concentration decreases (see Table 5).

4.6.4. Effect of pH

As follows from figure 9, pH, has an influence on the reduction of the simple metal ion. The effect of pH on the aquo nickel reduction was studied at constant ionic strength of 0.2M KNO_3, by adding sodium hydroxide.

The resulting change in the ionic strength due to the sodium hydroxide is negligible. Although no significant shift in the peak potential occurs a decrease in pH results in an increase in the peak current. This trend is also consistent for reductions carried in borate buffer, except for the peak potentials which are less negative at lower pHs (Table 6). The addition of the uncharged boric acid has no effect on the ionic strength, its effect being only on the pH of the medium.

Table 6. Variation of the Peak Potential and Peak Current of 2×10^{-4}M $NiSO_4$, in 0.06M borax, with Boric acid Concentration

$[H_3BO_3]$ M	pH	$i_p u$ Amps	$-E_p V$
-	9.2	0.33	1.07
0.4	8.4	0.48	1.06
0.8	7.2	0.63	1.04

The variation of the Ni(II) - threonine peak currents as a function of pH were studied for three different constant threonine concentrations. The pH was varied by adding boric acid into sodium tetraborate. The peak currents and potentials are given in tables (7), (8), (9). The prewave currents are plotted in Figure 11.

The trend of prewave peak current growth when the threonine concentration is $5x10^{-3}$M is in the reverse direction from that observed when the threonine concentration was $6.7x10^{-4}$M and 10^{-4}M. The prewave peak current increases to a maximum and then falls down. The peak potentials for both waves appear at more positive values with decreasing pH in all the systems, except for the system in which the threonine concentration is 10^{-4}M, where the prewave peak potential does not change.

Table 7. Variation of Peak Currents, and Potentials as a Function of pH for the systems, where $[Na_2B_4O_7]$ = 0.06M, $[Ni^{2+}]$ = $2x10^{-4}$M, [Thr] = 10^{-4}M

$[H_3BO_3]$ M	pH	i_{p_1} u Amps	$-E_{p_1}$ V	i_{p_2} u Amps	$-E_{p_2}$ V
-	9.2	0.5	0.94	0.274	1.07
0.1	8.85	0.511	0.94	0.376	1.07
0.2	8.4	0.458	0.94	0.456	1.066
0.4	7.8	0.29	0.94	0.496	1.06
0.6	7.2	0.176	0.94	0.54	1.05
0.8	6.8	-	-	-	-
Saturated	6	-	-	-	-

Table 8. Variation of Peak Currents, and Potentials as a Function of pH for the Systems, where $[Na_2B_4O_7]$ = 0.06M, $[Ni^{2+}]$ = $2x10^{-4}$M, [Thr] = $6.7x10^{-4}$M

$[H_3BO_3]$	pH	i_{p_1}	$-E_{p_1}$	i_{p_2}	$-E_{p_2}$
-	9.2	0.554	0.942	0.684	1.116
0.1	8.85	0.664	0.94	0.62	1.116
0.2	8.4	0.728	0.934	0.5	1.110
0.4	7.8	0.791	0.932	0.308	1.104
0.6	7.2	0.64	0.93	0.327	1.04
0.8	6.8	0.464	0.926	0.447	1.036
Saturated	6	0.196	0.928	0.62	1.03

Table 9. Variation of Peack Currents, and Potentials as a Function of pH for the Systems, where $[Na_2B_4O_7]$ = 0.06M; $[N_i^{2+}]$ = $2x10^{-4}$M, [Thr] = $5x10^{-3}$M

H_3BO_3	pH	i_{p_1}	$-E_{p_1}$	i_{p_2}	$-E_{p_2}$
-	9.2	0.044	0.96	0.812	1.124
0.1	8.85	0.074	0.952	0.876	1.12
0.2	8.4	0.148	0.952	0.904	1.114
0.4	7.8	0.392	0.933	0.786	1.11
0.6	7.2	0.72	0.926	0.502	1.04
0.8	6.8	0.874	0.922	0.292	1.092
Saturated	6	0.616	0.916	0.404	1.024

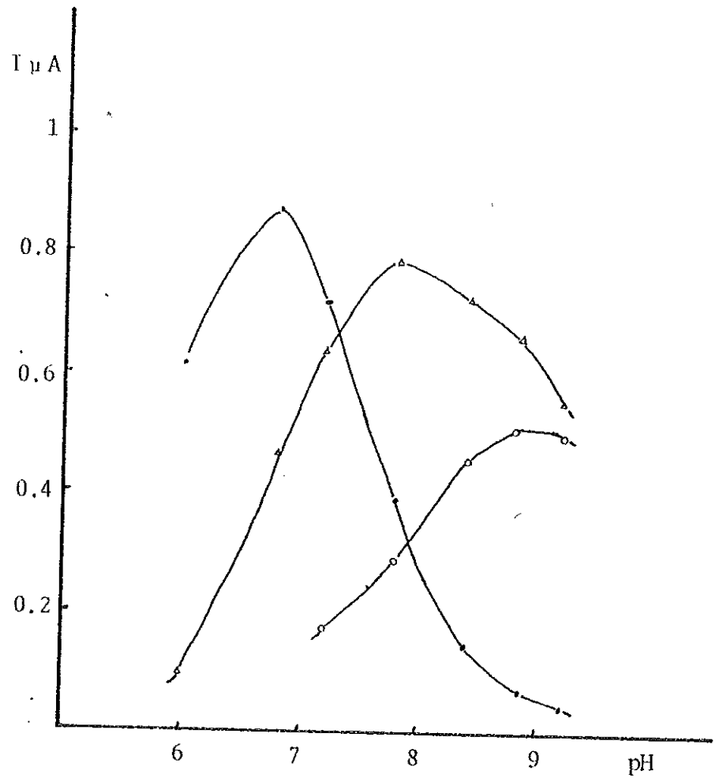

Figure 11. Plot of the variation of prewave peak current with pH for the system 0.2mM Ni(11), 0.06m borax and varying conc. of boric acid. threonine conc.,0.1(o), 0.67(Δ) and 5(·)mM.

4.6.5. Test of the Characteristics of the Prewave

In order to elucidate the mechanism of the polarographic reduction of the Ni(II) - threonine system, studies were made in 0.01M broax and threonine and metal concentrations of $2x10^{-4}$M each. Under these conditions, higher positive shifts of the peak potential and maximum prewave peak currents are observed. Because the prewave peak current is more than ten times that of the second wave, its DC polarogram is well developed. The reduction peak potential of Ni(II) in 0.01M borax is 0.988V and its peak current is 1 μamps, while that of the prewave when the threonine concentration is $2x10^{-4}$M is -0.924V and the peak current is 1.15 μamps. The second wave's peak potential is -1.042V and its peak current is 0.23 μamps (see Table 1).

To determine whether the electrode process is diffusion, kinetic or catalytic controlled, drop time and mercury reservoir height dependence of the limiting current were studied. The results are included in Table 10 and 11. Their corresponding figures are (12)and (13). The slopes of the log i versus log t, log i, versus log h, plots are 0.15 and 0.72 respectively.

Table 10. The Prewave Limiting Current Dependence on the Mercury Reservior Hight for the System $2x10^{-4}$M threonine $2x10^{-4}$M Ni(II),0.06M borax

log h	-log id
1.4814	0.2924
1.5587	0.2487
1.6149	0.2048
1.6646	0.1765
1.7093	0.1537
1.7868	0.0867
1.8525	0.0372
1.882	0.9177

Table 11. The Prewave Limiting Current Dependence on Drop Time for the System: $2x10^{-4}$M Threonine $2x10^{-4}$M Ni(II), 0.06 Borax

log t	$-\log id_1$
0.146	0.2048
0.30103	0.1884
0.4771	0.14996
0.6021	0.1463
0.699	0.1319

The drop time versus potential curves of the DME in 0.09M KNO_3, 0.03M borax, and 0.09M KNO_3, 0.03M borax, $8x10^{-5}$M threonine are given in Figure 14. The presence of threonine in the solution has no effect on the drop time.

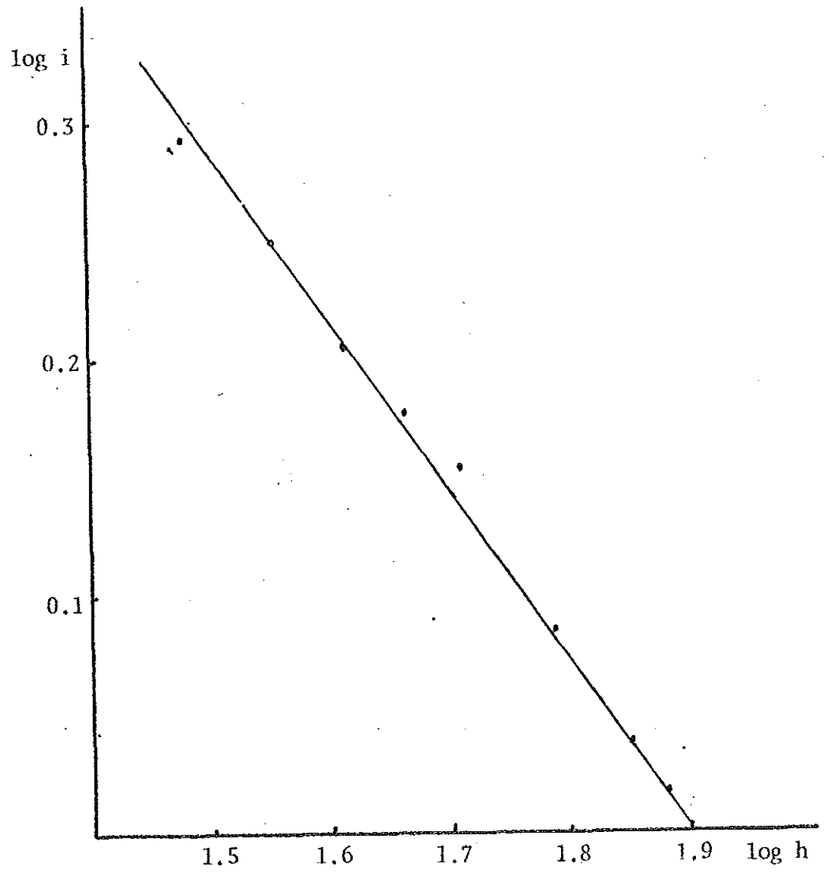

Figure 12. Plot of log i_{d_1} Vslog h for Ni(11) and threonine 0.2mM each in 0.06m borax.

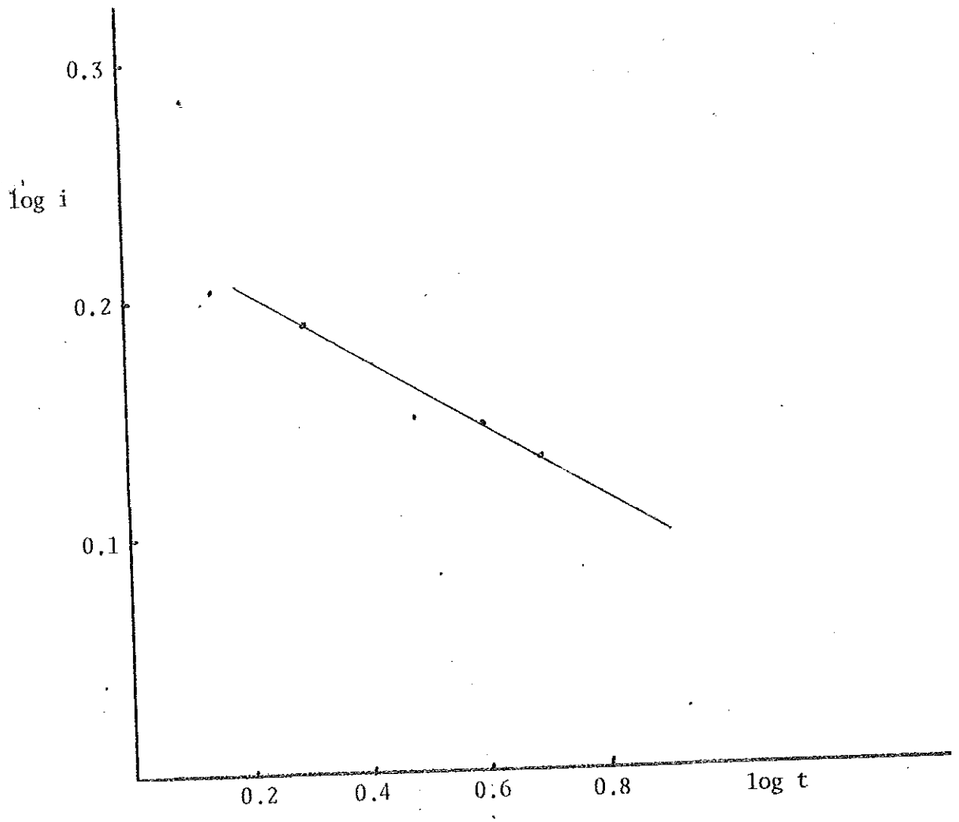

Figure 13. Plot of log i_1 Vs log t for Ni(II) and threonine 0.2mM each in 0.06m borax.

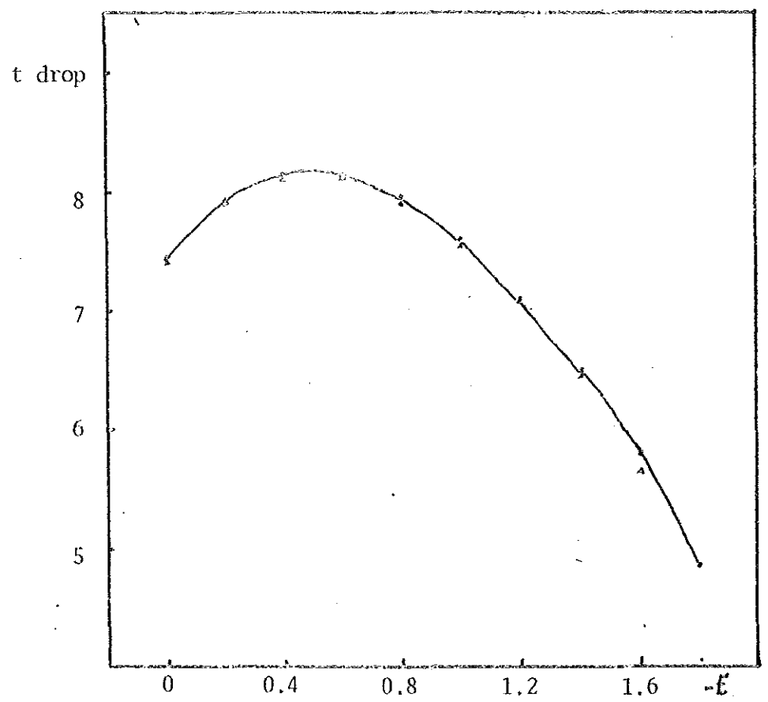

Figure 14. Droptime dependence on potential for 0.09m KNO_3, 0.03m borax(·), and 0.09m KNO_3, 0.03m borax, 0.05mM threonine(x).

4.7. Discussion

A study of the character of the Ni(II) - threonine double wave reveals the presence of two classes of species reducible at different potentials. Although, as cited earlier, adsorption can possibly lead to the splitting of a reduction wave, this may, however, be discounted in the present instance because of the non-appearance of an adsorption peak in the DC polarograms, droptime dependence on potential (see Figure 14) and the decrease of the peak current with increasing threonine concentration (see Figure 3 and 4) which are all contrary to the nature of an adsorption wave.

If the double wave is not caused by adsorption, then there must at least exist two electroactive specieses whose reduction potentials are different. Al low concentrations of threonine 1:17 ligand to metal ratio (see Table 3), a prewave and a second wave exist simultaneously. When the threonine concentration is relatively small the reduction potential of the second wave is the same as that of the simple metal ion (see Table 3 and Figure 10).

Figure 1 clearly shows the effect of threonine concentration in 0.01M borax. This condition is particularly suitable to follow the effect of threonine because the second wave's peak potential is more cathodic, and that of

the prewave peak potential is more anodic than that of the simple metal ion. At very low threonine concentration no prewave peak current occurs up to $8x10^{-5}M$ threonine, at which concentration the peak potential is shifted to a more positive potential (-0.946V). With increasing threonine concentration a second wave begins to appear, and the prewave peak current also increases. Prewave peak current stops to increase when the threonine concentration is greater than $2x10^{-4}M$ but less than $4x10^{-4}M$ (see Figure 3). A ratio of 1:1 threoninate to Ni(II) is achieved if the threonine concentration is $3.7x10^{-4}M$. At concentrations greater than $4x10^{-4}M$, the prewave peak current decreases. The most significant result is that the decrease of the prewave peak current is accompanied by an increase of the second wave peak current. The prewave peak current consistently decreases with increasing threonine concentration until at $8x10^{-3}M$ threonine, the prewave is almost non-existant (see Figure 1). The pH studies also show the same kind of phenomenon. At constant threonine concentration, changes in pH that result in an increase in the prewave peak current are also accompanied by a decrease in the second wave peak current and vise versa (see Tables 7, 8, and 9).

If at very low threonine concentration (when the ligand to metal ratio is below one), a prewave exists (at a potential that does not correspond to the reduction

of the simple metal ion) and if, at very high threonine concentration, only the second wave exists, then it appears that the prewave must result from the reduction of Ni(II) - threonine complex of the least ligand number, namely $[Ni(thr)]^{+1}$, while the second peak must correspond to the reduction of the complexes with higher ligand numbers.

A solution containing an equilibrium mixture of metal complexes is normally expected to give rise to several polarographic reduction peaks, if the reductions are kinetically controlled (the reduction potentials of the complexes being different). The sum of the prewave and second wave currents exceeds that of the simple metal ion (see Tables 1, 2 and 3). This, however, leads to the conclusion that the reduction cannot be purely kinetically controlled since, if only kinetic and diffusion processes were involved, the sum of both waves should practically have been equal to that of the simple metal reduction current. Nevertheless both waves separately can even give higher currents than that of the simple metal ion reduction (see Figures 4 and 5). Therefore, there also exists some kind of catalytic process (exhibited through enhanced peak currents) in conjunction with the kinetic one.

It is known that Ni(II) complexes with two molecules of threonine and serine (10, 67, 64, 65). Ni(II) is most

unlikely to form $[Ni(thr)_3]^{-1}$. Infact the first stepwise stability constant is higher than the second, thereby exhibiting the decreasing tendency of further coordination. Ohnaka and Matsuda (23) have shown tha Ni(II) forms $[Ni(gly)_3]^{-1}$ (gly = glycine), when the glycine concentration is 0.05M at a pH of 9.2 and Ni(II) concentration of $4x10^{-5}$M. In the present work the second wave appears when the metal to ligand ratio is as low as 1:2 (see Table 11), a condition where formation of $[Ni(thr)_3]^{-1}$ is not at all feasible. Therefore it may be concluded that the prewave and second wave result from the reduction of one threonine and two threonine complexes of Ni(II).

The prewave in the polarographic reduction of the Ni(II) - threonine complex is strongly dependent on the concentration of threonine. This immediately suggests that the nature of the wave is catalytic and tha it is possible to use this wave for an indirect polarographic determination of threonine. Since threonine is polarographically non-reducible, the use of the prewave peak current for threonine determination is of analytical importance.

Conditions in which well resolved peaks and higher currents can be obtained were examined at different borax concentrations (see Figure 10). Although decreasing borax gives higher peak currents the resolution is poorer. A 0.09M KNO_3, 0.03M borax mixture supporting

electrolyte was found to be the most suitable. From Figure 7, the optimum Ni(II) concentration is 0.2mM, because higher concentrations do not cause a significant increase in the prewave current. In this system, i.e. 0.09M KNO_3, 0.03M borax, 0.2mM Ni(II), the prewave peak current linearly increases with increasing threonine concentration in the range 10^{-5} to $8x10^{-5}$M (see Figure 6).

4.8. Conclusions

The essential results of this study on the polarographic reduction of Ni(II) - threonine system are the following.

1. Two waves are obtained and the prewave is believed to be due to the reduction of the mono threonine complex of Ni(II), while the second wave is due to that of the reduction on $Ni(thr)_2$. The enhanced current magnitude of both waves is indicative of a catalytic prewaves. The following scheme is proposed for the mechanism of the reduction.

   At low threonine concentration:

   a. $Ni(II) - thr = [Ni(thr)]+$

   b. $Ni(thr)^+ + 2e = Ni(0) + thr$ (prewave)

   At high threonine concentration

   c. $[Ni(thr)^+ + thr = Ni(thr)_2$

   d. $Ni(thr)_2 + 2e = Ni(0) + thr$ second wave.

At intermediate concentrations of threonine, both $[Ni(thr)]^+$ and $Ni(thr)_2$ are believed to be in equilibrium with each other:

$$[Ni(thr)]^+ + thr^- \underset{\longleftarrow}{\overset{\text{slow}}{\longrightarrow}} Ni(thr)_2.$$

giving rise to two waves, corresponding to the reduction of $[Ni(thr)]^+$ and $Ni(thr)_2$.

The catalytic nature of the two waves, may be explained in terms of the following scheme:

Prewave $[Ni(thr)]^+ + 2e \longrightarrow thr_o^- + Ni(0)$

$$Ni^+(II)_o \xleftarrow{\text{diffusion}} [Ni(II)$$

second wave $Ni(thr)_2 + 2e \longrightarrow 2thr_o^- + Ni(0)$

$$[Ni(thr)]_o^+ \xleftarrow{\text{diffusion}} [Ni(thr)]^+$$

The overall mechanism of the electroreduction may thus be summarized as

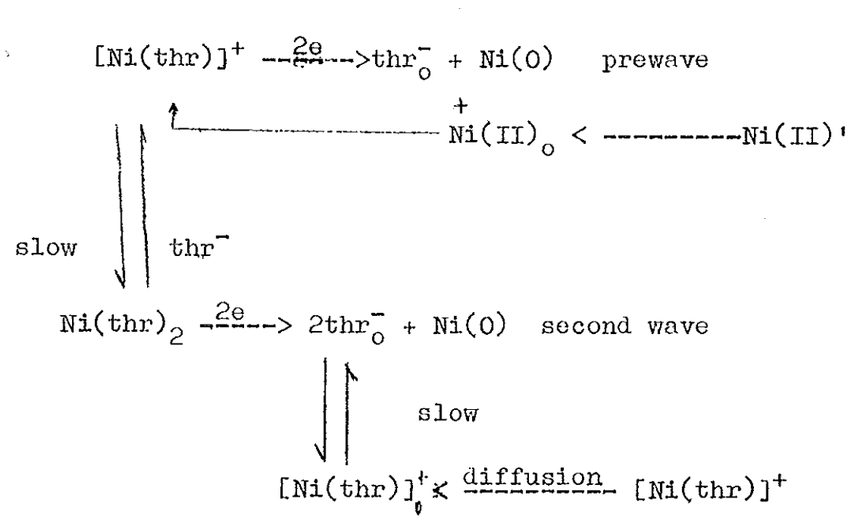

This mechanism is similar to the one proposed by several workers (15, 21, 29, 66). The subscript, zero, refers to the surface of the electrode.

2. The prewave peak current has been found to be u useful for the quantitative determination of threonine in the range 10^{-5} of $8x10^{-5}$M. The optimum condition is 0.2mM Ni(II), 0.09M KNO_3 and 0.03M borax.

5 . Summary

The polarographic reduction studies of the complexes of Cd(II), Co(II) and Ni(II) with threonine have shown that it is the anion form, i.e, the threoninate, that complexes. The reduction of Cd(II) as a simple metal ion and as complexes of threonine are polarographically reversible. The stepwise stability conctants have been calculated, using the Deford-Hume method. In these calculations the free ligand concentration has been calculated considering the pH effect on the relative proportions of the zwitterion and anion forms of threonine. The stepwise stability constants so obtained are log k_1 = 3.1 and log k_2 = 2.57.

Because of the high sensitive and resolution that can be obtained in differential pulse polarography, this technique was largely used in the study of Ni(II) and Co(II) complexes with threonine. Both cations seem to produce a series of complexes whose reduction potentials are separated enough to result in several peaks. The appearance of these peaks has been accounted for at least for the Ni(II) threonine system, by the slow equilibrium that exist between the complexes.

Ni(II) forms two distinct peaks at low and moderate threonine concentrations, whose reduction peak potentials are different from the aquonickel reduction peak. Both

peaks have shown catalytic nature. Although the threonine concentration dependence of the CO(II) reduction peak has shown a catalytic nature, similar to the Ni(II) - threonine systen, it has not been supported by the log i - log t, log i - log h dependence studies.

From the non-appearance of an adsorption peak in the dc polarograms, a decreasing of the peak current with increasing complex concentrations, as well as from the reservoir height and droptime dependences of the liniting currents, adsorption has been discounted as being involved in the polarographic reductions of the complexes.

Although no kinetic studies were made, the increase of the peak currentwith increasing threonine concentration. accompanied by the anodic shift of the Co(II) - threonine reduction potential, can be a consequence of the transition of the reduction from an irreversible to a reversible one, as is also apparent from the half peak widths.

The double wave of Ni(II) - threonine system has been shown to result from $[Ni(thr)]^+$ and $Ni(thr)_2$ reductions. The splitting of the waves has been accounted by the existence of a relatively slow equilibrium between these complexes in comparison to the electrode reduction rate. A scheme for the mechanism of the process has been given.

The catalytic prewave peak current has been shown to be useful for the quantitative polarographic determination of threonine. The optimum condition is 0.2mM Ni(II), 0.09m KNO_3 and 0.03M borax. Under this condition the peak current dependence on threonine is linear over a range of 10^{-5}M to $8x10^{-5}$M.

References

1. J.J. Lingane, Chem. Revs., (1941) 10.
2. D.D. Deford and D.N. Hume, J. Am. Chem. Soc., 73
3. C.G. Butler and R.C. Kaye, J. Electroanal. Chem., 8 (1964) 463.
4. M.E. Macovshi, J. Electroanal. Chem., 16 (1968) 457.
5. N.G. Elenkova and T.K. Nedelcheva, J. Electroanal. Chem., 69 (1976) 395.
6. J. Biernat and M. Branowska - zralka, Electrochim. Acta, 17, (1972) 1867.
7. W.B. Schapp and D.C. McMasters, J. Am. Chem. Soc., 83 (1961) 4699.
8. J. G. Sullivan and J.C. Hindman, J. Am. Chem. Soc., 74 (1952) 6091.
9. P.C. Rawat and C.M. Gupta, Ind. J. Chem. 11 (1973) 186.
10. S.T. Chow and C.A. McAuliffe, Progress in Inorganic Chem., Vol. 19 S.J. Lippard (ed.), 1975, John. Wiley, New York.
11. A.A. Vicek, Nature, 180 (1957) 753.
12. Im. Kolthoff and J.J. Lingane, "Polarography", Interscience Publishers, New York, 2nd ed. pp 257.
13. K. Yokoi, T. Ozek, I. Watanabe and S. I. Keda, J. Electroanal. Chem., 132 (1982) 191.
14. H.B. Mark. Jr., J. Electroanal. Chem., 7 (1964) 276
15. H.B. Mark. Jr. and C.N. Reilley, J. Electroanal. Chem., 4 (1962) 189.

16. Ya. I. Tur yan and O.E. Ruvinskii, J. Electroanal. Chem., 23 (1962) 61.

17. S. Minc and J. Andrzejczak, J. Electroanal. Chem., 17 (1968) 101.

18. A. Calusaru and V. Voicou., J. Electroanal. Chem., 32 (1971) 427.

19. H.B. Mark Jr., and H.G. Schwartz Jr., J. Electroanal. Chem., 6 (1963) 443.

20. L. Meites, "Polarographic Techniques" Inter Science Publishers Inc., New York. 1965 pp. 187-189.

21. P. Mader, Coll. Czech. Chem. Comm., 36 (1971) 1035.

22. K. Kustin, R.F. Pasternack, and E.M. Weinstock, J. Am. Chem. Soc., 88.

23. N. Otlnaka, H. Matsuda, J. Electroanal. Chem., 62 (1975) 245.

24. G.G. Hammes, et al., J. Am. Chem Soc., 84 (1962) 4639.

25. C. Nishihara, H. Matsuda, J. Electroanal. Chem., 28 (1970) 17.

26. D.A. Alekenes, Pushpanaden, Electrochem. Acta., 27 (1982) 365.

27. I.V. Nelson and R.T, Iwamato, J. Electroanal. Chem., 6 (1963) 234.

28. R.E. Connick and Coppel, J. Am. Chem Soc., 81 (1959) 6839.

29. J. Galvez, D. Maria, T. Fuente and M. Sarabia, Electrochem. Acta., 27 (1982) 1253.

30. Cosovic and Markobranica, J. Electroanal. Chem., 20 (1969) 269.

31. E. Etabashi., J. Electroanal. Chem., 89 (1978) 205.

32. I.M. Klthoff, P. Mader, S.E. Khalafalla, J. Electroanal. Chem., 18.

33. H.B. Mark Jr., and C.N. Reilley, Anal. Chem., 35 (1963) 195.

34. I.M. Kolthoff and J.J. Lingane, "Polarography" Inter-Science Pub. Inc., 2nd ed., New York, p. 481.

35. W. Gorski and J. Lipkowski, J. Electroanal. Chem., 133., (1982) 253.

36. I.M. Kolthoff and J.F. Coetzee, J. Am. Chem. Soc., 79 (1957) 870.

37. I.M. Kolthoff and J.F. Coetzee, J. Am. Chem. Soc., 79 (1957) 1852.

38. E. Eriksrud, J. Electroanal. Chem., 90 (1978) 347.

39. F. Basolo and R.G. Pearson., "Mechanisms of Inorganic Reactions" 2nd ed., Wiley Eastern Pr. Ltd., 1973 and References cited therein.

40. J. Dandoy and L. Gierst, J. Electroanal. Chem., 2 (1961) 116.

41. R. Bennes, J. Electroanal. Chem., 44 (1973) 145.

42. N.S. Hush and J.W. Scarrett, J. Electroanal. Chem., 7 (1964) 26.

43. I.M. Kolthoff and J.J. Lingane, "Polarography" 2nd ed., 1955, Interscience Pub. New York.

44. A.A. Vecek, Z. Electrochem., 61 (1957) 1014.

45. U. Tanaka, R. Tamamushi and M. Kadama, Bull. Chem. Soc. Japan, 33 (1960) 14.

46. W.C. Purdy "Electroanalytical methods in Biochemistry" McGraw-Hill Inc. New York (1965).

47. D.M. Gruen and R.I McBeth, J. Phys. Chem., 63 (1959) 393.

48. W. Manch and W.C. Fernclius, J. Chem. Educ., 38 (1961) 192.

49. R.C Larson and R.T. Iwamato, J. Am. Chem. Soc., 82 (1960) 3239.

50. G. Zotti and G. Pilloni, J. Electroanal. Chem., 124 (1981) 277.

51. R.C. Larson and R.T. Iwamato, J. Am. Chem. Soc., 82 (1960) 3239.

53. E.H. Lyons, Jr., J. Electrochem. Soc., 101 (1954) 376.

54. P. Mader, I.M. Kolthoff, J. Polarog. Soc., 14 (1968)42.

55. A.A. Vlcek "Progress in Inorganic Chemistry," Vol.5, F.A. Cotton, Ed., Interscience, New York, 1963, pp. 211.

56. Z. Galus, "Fundamentals of Electrochemical Analysis", Ellis Horwood, 1976, Chap. 8.

57. L. Meites, "Polarographic Techniques," Interscience Publishers Inc., New York, 1965 p. 178.

58. J.C. Cassate and R.G Wilkeas., J. Am Chem. Soc., 90 (1968) 6045.

59. K. Kustin, R.F. Pasternack and E.M. Weinstock, J. Am Chem. Soc., 88 (1966) 4610.

60. A.F. Pearlmutter and J. Stuehr, J. Am. Chem. Socl, 90 (1968) 858.

61. W.F. Stack, A.F. Pearl Mutter and J. Stuehr, J. Am. Chem., 91 (1969) 4083.

62. W.C. Purdy "Electroanalytical Methods in Biochemistry," McGraw-Hill Inc., New York (1965) pp. 163-174.

63. E.V. Raju and H.B. Mathur, J. Inorg. Nucl. Chem., 30 (1968) 2181.

64. A. Gergely, I. Sovago, I. Nagypal, and R. Kiraly, Inorg. Chem. Acta., 3 (1972) 435.

65. A. Gergely, J. Mojzes and Zs. Kassai - Bazsa, J Inorg. Nucl. Chem., 34 (1974) 1277.

66. J.M. Lopez Fonseca and M.C. Arredondo., An. Quium. 78A (1982) 108.

67. J.M. Lopez and M.C Arredondo, Analyst, 107 (1982) 107.

68. D. Ilkovic, J. Chim. Phys., 35 (1939) 129.

69. J.J. Lingane and B.A. Loveridge, J. An. Chim. Soc., 72(1950) 438.

70. Z. Galus, "Fundamentals of Electrochemical Analysis" Ellis Horwood, 1976, Chap 5.

71. J. Koutecky., Colln. Czech. Chem. Commun., 18 (1955) 311.

72. J. Weber and J. Koutecky., Colln Czech Chem. Commum., 20 (1955) 980.

73. K. Wiesner., Z. Electrochem., 49 (1943) 164.

74. R. Bridicka and K. Wiesner., Colln. Czech. Chem. Commun., 12 (1947) 138.

75. J. Koutecky and R. Bridicka., Colln Czech. Chem. Commun., 12 (1947) 337.

76. J. Koutecky., Chem. Listy., 47 (1953) 323.

77. J. Koutecky., Chem. Listy., 47 (1953) 9.

78. L. Meites., "Polarographic techniques" Wiley, New York, 2nd ed. 1965, Chap. 10.

79. A.J. Bard and L.R. Faulkner, "Electrochemical Methods", Wiley, 1980, Chap 5.

80. Z. Galus., "Fundamentals of Electrochemical Analysis" Ellis Horwood, 1976, Chap. 20.

81. A.M. Bond and D.R. Canterford, Anal. Chem., 44(1972) 721.

82. G.A. Heath and G. Hefter, J. Electroanal. Chem., 84 (1977) 295.

83. A.M. Bond J. Electroanal. Chem., 20 (1969) 223.

84. E.P. Parry and R.A. Osteryoung., Anal. Chem., 37 (1965) 1635.